A persistent behavioral state enables sustained predation of humans by mosquitoes

Trevor R. Sorrells[1,2*], Anjali Pandey[1], Adriana Rosas-Villegas[1], and Leslie B. Vosshall[1-3*]

[1]Laboratory of Neurogenetics and Behavior, The Rockefeller University, New York, NY 10065 USA, [2]Kavli Neural Systems Institute, New York, NY 10065 USA, [3]Howard Hughes Medical Institute, New York, NY 10065 USA. Current Address: Department of Biology, Brandeis University, 415 South Street, Waltham, MA 02453 United States (A.P.). For correspondence: trevorsorrells@gmail.com, leslie.vosshall@rockefeller.edu

Abstract Predatory animals pursue prey in a noisy sensory landscape, deciding when to continue or abandon their chase. The mosquito *Aedes aegypti* is a micropredator that first detects humans at a distance through sensory cues such as carbon dioxide. As a mosquito nears its target it senses more proximal cues such as body heat that guide it to a meal of blood. How long the search for blood continues after initial detection of a human is not known. Here we show that a 5-second optogenetic pulse of fictive carbon dioxide induced a persistent behavioral state in female mosquitoes that lasted for more than 10 minutes. This state is highly specific to females searching for a blood meal and was not induced in recently blood-fed females or in males, who do not feed on blood. In males that lack the gene *fruitless*, which controls persistent social behaviors in other insects, fictive carbon dioxide induced a long-lasting behavior response resembling the predatory state of females. Finally, we show that the persistent state triggered by detection of fictive carbon dioxide enabled females to engorge on a blood meal mimic offered up to 14 minutes after the initial 5-second stimulus. Our results demonstrate that a persistent internal state allows female mosquitoes to integrate multiple human sensory cues over long timescales, an ability that is key to their success as an apex micropredator of humans.

Introduction

Predatory animals first detect, then pursue, and ultimately capture prey (**Endler, 1991**). Because the pursuit phase can last for extended periods of time, it is critical for predators to persist in the chase even when the prey is not constantly detected. It is equally important for predators to abandon pursuit if enough time has elapsed that prey capture is unlikely to occur. This decision balances the need to obtain food with the expenditure of energy on unsuccessful hunts (**Anholt et al., 1987, Williams et al., 2014**). The duration of a pursuit could depend on the predator repeatedly sensing prey stimuli. Alternatively, it may be sustained by recent prior experience or a change in the internal state of the predator that outlasts individual prey stimuli.

Micropredators such as the mosquito consume small quantities of their live prey rather than killing them outright (**Lafferty et al., 2002**), but employ similar tactics to other pursuit predators. Female mosquitoes combine rich multisensory information from olfactory, visual,

taste, mechanosensory, and contact chemosensory systems to hunt humans from whom they obtain blood to produce eggs. Carbon dioxide (CO_2) produced by human breath is highly volatile, traveling long distances from the human host. Detection of CO_2 by the mosquito results in an increase in flying behavior (**Eiras et al., 1991, McMeniman et al., 2014**) and upwind flight (**Dekker et al., 2011, Dekker et al., 2005, Geier et al., 1999**) that is often referred to as "activation". It has not been tested whether repeated sensory input from the host or reafferent signals of wind caused by flight are required to maintain this activation behavior.

Mosquitoes require an additional, more proximal host cue such as body heat or skin odor for short-range attraction and to engorge on blood (**Corfas et al., 2015, Dekker et al., 2011, Dekker et al., 2005, Geier et al., 1999, McMeniman et al., 2014, van Breugel et al., 2015**) (Figure 1A). In natural settings, human sensory cues are typically brief and intermittent by the time they reach the mosquito due to turbulent air flows and long distances (**Koehl, 2006**). However, studies of insect navigation have documented only short-term responses to these stimuli on the order of a few seconds (**Álvarez-Salvado et al., 2018, Dekker et al., 2011, Demir et al., 2020, Pang et al., 2018**). If mosquitoes possess the ability to retain information about their prey and combine it with future information this may explain their success at locating and feeding on human blood. Although the short-term role of CO_2 in mosquito behavior has been known for nearly 100 years (**Rudolfs, 1922**), the idea that CO_2 induces a long-term change in the internal state of the mosquito has not previously been tested experimentally.

To study pursuit predation in the mosquito, we developed optogenetic tools to precisely deliver short pulses of fictive CO_2. This allowed us to test the effect of activating CO_2 sensory neurons with greater temporal resolution and without the continuous stimulus of air flow required for delivery of real CO_2. We observed that detection of fictive prey led to a long-lasting behavioral change in female mosquitoes. Following a 5-second fictive CO_2 stimulus, animals exhibited high-arousal behaviors and engorged on a blood meal mimic offered up to 14 minutes later. Neither males nor previously blood-fed females showed these effects, and this persistent internal state was not induced by optogenetic stimulation of a sweet taste pathway. Remarkably, males lacking the *fruitless* gene showed long-lasting responses to fictive CO_2 resembling those in females, consistent with our prior observation that these mutants show some aspects of female mosquito behavior (**Basrur et al., 2020**). Our work identifies a persistent internal state that may explain how mosquitoes aggressively pursue human hosts for many minutes. This constitutes the first use of optogenetics to manipulate neural circuits in the mosquito, an advance that will enable a better understanding of this important disease vector.

Results

Fictive CO_2 triggers blood feeding

We created optogenetic tools in *Aedes aegypti* mosquitoes that allowed us to precisely activate sensory neurons that are specialized to detect CO_2. To do this we generated a transgenic strain that expresses the red light-activated cation channel CsChrimson translationally fused to the tdTomato fluorescent reporter (**Klapoetke et al., 2014**) under control of the *QF2/QUAS* bipartite transcription system (**Potter et al., 2010**). We crossed this transgene into a strain that expresses the QF2 transcription factor in neurons that express the

Gr3 CO_2 receptor subunit (**McMeniman et al., 2014, Younger et al., 2022**) (Figure 1B). CsChrimson-tdTomato was detected in maxillary palp neurons but not antennal neurons, consistent with the observation that maxillary palp neurons are exquisitely sensitive to CO_2 (**Grant et al., 1995**) (Figure 1C,D, Figure 1—figure supplement 1A). As expected, we found that CsChrimson-expressing neurons extended axons that innervated glomerulus MD1 in the antennal lobe of the mosquito brain (Figure 1E), which is known to be CO_2-sensitive (**Younger et al., 2020**). To test whether mosquitoes responded to optogenetic activation of CO_2 sensory neurons, we presented animals with a 5-second red light (627 nm) stimulus and tracked their movement (Figure 1F-I). Control animals carrying only the *Gr3-QF2* driver or the *QUAS-CsChrimson* transgene reporter showed no response to red light. However, mosquitoes with both genetic elements (*Gr3 > CsChrimson*) increased their velocity in response to the stimulus (Figure 1H-I). The proportion of mosquitoes responding increased with light intensity (Figure 1—figure supplement 1B-D). The observed increase in activity is consistent with the known role of CO_2 in activating mosquitoes.

When combined with another host cue such as heat, CO_2 is sufficient to elicit blood feeding in female mosquitoes (**McMeniman et al., 2014**). To test whether fictive CO_2 sensation triggered by optogenetic activation of *Gr3* sensory neurons could replace real CO_2, we created a behavior assay called the opto-membrane feeder (Figure 1J). This assay consists of a cylindrical canister of mosquitoes surrounded by red light-emitting diodes (LEDs) and a warm blood meal behind a membrane sitting on top of the mesh lid. Mosquitoes were presented with either CO_2, fictive CO_2 via red light, or neither stimulus. Control mosquitoes with either *Gr3-QF2* or *QUAS-CsChrimson* were attracted to the warm blood meal and engorged only when presented with CO_2 but not when presented with red light (Figure 1K-M). In contrast, *Gr3 > CsChrimson* mosquitoes were attracted and engorged in the presence of either real or fictive CO_2, the latter delivered as a red-light stimulus (Figure 1K-M). These results demonstrate that mosquitoes interpreted optogenetic activation of the CO_2 sensory neurons as a host cue that is sufficient to drive blood feeding.

Fictive CO_2 induces prolonged host-seeking behaviors

Host-seeking begins when female mosquitoes detect a human, typically by sensing volatile cues like CO_2. Once activated by human odorants, they seek out the source of the cues, and upon landing, mosquitoes walk to locate a patch of skin to pierce (**Liu et al., 2019, McMeniman et al., 2014, van Breugel et al., 2015**)). To understand the timing and nature of the mosquito response to transient host cues, we created an assay called the opto-thermocycler (Figure 2A-B). In this assay mosquitoes receive optogenetic light stimulation from above and heat through the mesh at the bottom of the assay chamber. The use of fictive CO_2 delivered optogenetically was critical for studying the internal state of the mosquito after these transient host cues. Delivery and removal of real CO_2 necessitates constant air flow, which is itself an important sensory cue for insects (**Álvarez-Salvado et al., 2018, Kadakia et al., 2021, Suver et al., 2019**).

We employed machine-learning based behavior classification as a high-throughput readout of mosquito behavioral responses (Figure 2C-D). We tracked nine points on the mosquito body using Animal Part Tracker and four behaviors using JAABA (**Kabra et al., 2013**): grooming, flying, walking, and probing, a behavior in which the mosquito inserts its proboscis through the

mesh in the bottom of the container. When none of these four behaviors were present, mosquitoes were predominantly motionless, showed slow hindleg movement, or occasionally flailed against the wall of the assay chamber without walking. All classifiers showed high accuracy with >90% true positive and true negative rates on a set of test video frames (Figure 2 – source data 1).

We delivered 5-second red light pulses and heat increases to simulate brief CO_2 and human body heat stimuli (Figure 2B). Mosquitoes responded to individual heat and fictive CO_2 stimuli with elevated walking, flying, and probing (Figure 2E-H, Figure 2—figure supplement 1). The response to heat alone was dominated by probing and returned to baseline after about one minute ($t_{1/2\ probing}$ = 0.4 minutes). In contrast, fictive CO_2 alone caused an immediate flight and probing response followed by sustained walking, flying, and probing (Figure 2H, Figure 2—figure supplement 1, Video 1) that took approximately 15 minutes to return to baseline ($t_{1/2\ probing}$ = 3.9 minutes). Varying the light intensity changed the proportion of mosquitoes responding but not the duration of the response (Figure 1—figure supplement 1B-D). The long duration of the response to CO_2 is reminiscent of persistent internal states in other organisms (**Asahina et al., 2014, Flavell et al., 2013, Hindmarsh Sten et al., 2021, Marques et al., 2020**).

These observations of mosquito behavior could reflect an internal state specific to host seeking or a general arousal state elicited by many sensory stimuli. Like CO_2, bright light is also an arousal signal in mosquitoes (**Araripe et al., 2018**) so we asked whether bright light induces a long-lasting behavior state. Mosquitoes have weaker visual sensitivity to red wavelengths (**San Alberto et al., 2021**), and we saw no behavioral response to red light (Figure 2E), so we used green light. Because this experiment is designed to test whether mosquitoes have a response to a visual stimulus, a question that does not depend on the use of optogenetics, we used wild-type mosquitoes. A bright green light stimulus induced a brief response dominated by walking ($t_{1/2\ walking}$ = 0.4 minutes), much shorter than the response to fictive CO_2 (Figure 2I,K).

While CO_2 and heat elicit the blood-feeding program required for females to produce eggs, mosquitoes possess a second, distinct feeding program for ingestion of flower nectar for energy (**Jové et al., 2020, Lahondere et al., 2020**). We asked whether optogenetic stimulation of *Gr4* sensory neurons that are thought to detect sugar evoked a sustained behavior response in mosquitoes as with optogenetic activation of the CO_2 sensory neurons. We found that fictive sugar elicited a response composed largely of probing that was of shorter duration than fictive CO_2 ($t_{1/2\ probing}$ = 1.5 minutes) (Figure 2J,L).

The temporal resolution of our assays allowed us to understand precisely how mosquitoes integrate CO_2 and heat to affect their behavior. We focused on the first 15 seconds after stimulus onset during which the greatest behavior responses are seen. We found that the heightened probing response seen when the stimuli were presented together was roughly additive with respect to the individual stimuli (Figure 2M, Figure 2—figure supplement 2). In contrast, flying was strongly suppressed. This demonstrates that multimodal integration of host cues biases action selection away from long-range flight and toward a short-range probing behavior.

Heat is a host cue but also may be experienced by the mosquito under other environmental contexts. We compared the integration of heat with green light and fictive sugar to see if they are integrated similarly to the host cue CO_2. In contrast to the integration of host cues, probing was suppressed when non-host cues were presented together (Figure 2M, Figure 2—figure supplement 2). This demonstrates that the mosquito nervous system uses different computations for the integration of host cues and non-host cues.

The CO_2-evoked persistent state is specific to host seeking

The fact that bright green light and fictive sugar stimuli elicited briefer responses suggested that the prolonged response to fictive CO_2 is specific to host seeking. If true, it should be modulated similarly to host-seeking behavior. Host seeking in *Aedes aegypti* is suppressed after a female takes a blood meal, only returning after she lays eggs several days later (**Duvall et al., 2017, Klowden, 1981**). We allowed female mosquitoes to blood feed on a human arm and then assayed their behavior four days later. We found that blood-fed females completely lost their response to fictive CO_2 and nearly completely lost their response to heat (Figure 3A,B,D,E). For comparison, we asked whether blood-fed females could respond to the optogenetic sugar stimulus by activating *Gr4* sensory neurons. We found that blood-fed females had reduced responses to fictive sugar, but unlike fictive CO_2, the response was still detectable (Figure 3—figure supplement 1A-E). This demonstrates that blood-fed females specifically show a complete loss of the persistent state elicited by fictive CO_2.

Unlike females, male mosquitoes do not seek out hosts to feed on blood. Males do demonstrate a flight response to CO_2 (**Matthews et al., 2016**) and are reported to congregate in the vicinity of humans where they mate with female mosquitoes (**Hartberg, 1971**). We observed that male mosquitoes had minimal responses to heat, but substantial flight and walking responses to fictive CO_2 (Figure 3C-E). However, the response to fictive CO_2 was brief, decaying rapidly back to baseline ($t_{1/2\ probing}$ = 0.4 minutes). This observation suggests that the persistence—but not the initial response—is specifically regulated in a sexually dimorphic manner.

We have previously shown that *fruitless* mutant male mosquitoes gain strong attraction to human odor (**Basrur et al., 2020**). We asked whether these *fruitless* mutant males have an altered response to fictive CO_2 stimuli. First, we confirmed that *fruitless* mutant males lacking *Gr3 > CsChrimson* did not respond to red light, as expected (Figure 3F). *fruitless* heterozygotes receiving fictive CO_2 showed a brief response ($t_{1/2\ probing}$ = 0.4 minutes) (Figure 3G,I,J), similar to the response we saw for wild type males (Figure 3C). By comparison, *fruitless* mutant males receiving fictive CO_2 showed a strong and sustained response for minutes after the stimulus ($t_{1/2\ probing}$ = 1.7 minutes) (Figure 3H-J). This suggests that *fruitless* is involved in the regulation of the sexual dimorphism of the persistent host-seeking state. We note that the duration of the sustained response of *fruitless* mutant males is shorter than in females, suggesting additional sexually dimorphic factors may regulate this internal state. Taken together, these results demonstrate that blood-fed females and males, which do not engage in blood-feeding behavior, lack sustained responses to brief pulses of fictive CO_2. This raises the possibility that the persistent state is the behavioral mechanism by which the goal of blood feeding is sustained in the female mosquito.

Mosquitoes integrate sensory cues for minutes

Motivation consists of two components: increased arousal and directed action toward a goal. We have demonstrated that fictive CO_2 induces a prolonged increase in movement and the probing behavior that immediately precedes blood feeding. We asked whether the persistent state induced by a brief pulse of fictive CO_2 can influence the response to body heat and ultimately if it can induce blood feeding many minutes afterwards.

First, we tested whether fictive CO_2 primes subsequent responses to heat (Figure 4A). Because CO_2 is highly volatile, mosquitoes likely sense this cue before body heat in naturalistic host-seeking settings. When we presented heat first followed by fictive CO_2, relatively small behavioral responses were evoked (Figure 4B-C). However, when fictive CO_2 was presented simultaneously with heat or 15 or 60 seconds prior to heat, larger walking and probing responses were seen (Figure 4B-C). This suggests that mosquitoes respond most strongly to the naturalistic temporal order of these host cues. Next, we asked how long prior to the heat stimulus fictive CO_2 can boost the response (Figure 4D). Compared to heat alone, walking and probing were increased when a fictive CO_2 stimulus was presented up to four minutes prior (Figure 4E-F). This demonstrates that in addition to the sustained behavior response, fictive CO_2 increases the response to heat for minutes afterward.

Once a mosquito pierces the skin of a human host, taste cues present in the blood guide the decision to engorge. Because this is the final goal of host-seeking behavior, we wondered whether mosquitoes in the fictive CO_2-triggered persistent state had altered responses to both heat and taste stimuli. To test this, we designed a blood blanket assay that incorporated a thin sheet of a blood meal mimic located between the thermocycler heating element and the mesh below the mosquito, allowing it to be rapidly heated and cooled (Figure 4G-H). We used a solution of ATP in saline, which has previously been shown to be a highly palatable meal that induces females to engorge in the same manner as blood (**Galun et al., 1963, Jové et al., 2020**). This allowed us to test how the prolonged arousal state induced by fictive CO_2 influences the decision of the mosquito to feed on a blood meal mimic.

First, we explored the temporal relationship of host stimuli to test whether the naturalistic order of CO_2, heat, and taste stimuli elicits greater rates of feeding. When fictive CO_2 was presented along with heating of the meal for 10 minutes, many females fed to repletion (Figure 4I). To test the temporal order of these cues, we offered fictive CO_2 and a meal that was only warmed for several minutes, resulting in reduced feeding levels (Figure 4I). When the order was swapped and females were briefly offered the warm meal prior to fictive CO_2, very few females fed (Figure 4I). This suggests that mosquitoes feed at the highest rates when they receive a CO_2 stimulus prior to heat and taste stimuli.

Next, we asked how long after a brief pulse of fictive CO_2 females would retain the motivation to feed on the blood meal mimic. When offered the warm meal without fictive CO_2, few females fed. We then stimulated the females with fictive CO_2 and heated the blood meal mimic either immediately or after a delay of 2, 8, 14, or 20 minutes after fictive CO_2. We hypothesized that if the fictive CO_2 induced a persistent state of host seeking, it might trigger engorging behavior many minutes later. Indeed, fictive CO_2 was able to potentiate feeding when presented up to 14 minutes prior to heating of the blood meal mimic (Figure 4J). Taken together, our results

demonstrate that the persistent host-seeking state increases host-seeking behaviors and alters the response to sensory cues for many minutes after a brief fictive CO_2 stimulus. We speculate that this reflects the amount of time a mosquito will pursue a host in a naturalistic setting before halting the search if it appears that the host is no longer nearby.

We noticed that there is considerable individual variation in how mosquitoes respond to the warm blood meal mimic after being activated by fictive CO_2 (Figure 4J). We asked whether the behavior state of individual mosquitoes could be inferred over longer periods of time. We extracted 38 behavior parameters from the experiment in Figure 4J from 30-second-long time windows and used t-distributed stochastic neighbor embedding (tSNE) to visualize the relationships. This embedding revealed that mosquito behavior fell into four major states that we termed rest, global search, local search, and engorge (Figure 4K, Figure 4—figure supplement 1). These states were observed even when the length of the time window was varied over a 6-fold range (Figure 4—figure supplement 2). The states differed in the proportions of behaviors observed, the transition rates between them, and the total distance the mosquito travelled while in each state. We divided the data into those females that eventually fed or did not feed at the end of the experiment (Figure 4L). As expected, the engorge state was greatly enriched in mosquitoes that were categorized as fed, demonstrating that this method is effective at identifying longer-timescale behavior states (Figure 4L).

We asked whether the behavior state of the mosquito after fictive CO_2 was associated with the future decision to feed on the warm blood meal mimic. We found that fed and unfed mosquitoes showed similar amounts of global search pre-heat but greater levels of local search for those that would later feed (Figure 4M). The local search state differs primarily by showing more probing and less flight than the global search state. To avoid potential distortions created by the 2-dimensional embedding (**Chari et al., 2021**), we trained a linear classifier using only the four behaviors (groom, walk, flight, and probe). A classifier trained on the proportion of time mosquitoes spent in each behavior for 2 minutes after the light stimulus could predict which mosquitoes would later feed with above-chance accuracy (Figure 4N). Thus, the behavior state that individual mosquitoes enter in response to fictive CO_2 reflects the likelihood of response to future sensory cues.

Discussion

We investigated how female mosquitoes pursue humans by combining multisensory stimuli in time to achieve the goal of feeding on human blood. To precisely control the delivery of CO_2, we generated optogenetic tools to deliver fictive CO_2 and combined this with high-resolution behavior assays and machine learning analysis approaches. These experiments demonstrated that optogenetic activation of CO_2 sensory neurons induced a long-lasting behavior state change (Figure 4O). During this time mosquitoes had heightened responses to heat and were more likely to feed on a blood meal mimic even if encountered minutes after the CO_2 stimulus.

Integration of sensory information over time allows the nervous system to optimize decision making for a particular goal (**Körding, 2007**). Testing whether predators use this approach during hunting requires a precise understanding of what the predator is sensing and when, precluding field studies. Laboratory studies have found behavior responses altered for as long as a few seconds after encountering CO_2 in mosquitoes and other olfactory stimuli in

Drosophila (**Álvarez-Salvado et al., 2018, Dekker et al., 2011, Demir et al., 2020, Pang et al., 2018**). Although this timescale of sensory integration is sufficient for upwind tracking, modelling suggests that integration over long timescales can maximize the information about the location of an olfactory stimulus (**Vergassola et al., 2007**). Here, we show that mosquitoes integrate olfactory, heat, and taste stimuli for at least 14 minutes, much longer than previously assumed. The increased movement and the bias of actions toward a particular goal constitute an internal motivational state sustained over minutes—one specific to feeding on humans. Importantly, our results show that this internal state does not require constant flight behavior or a constant air flow stimulus, demonstrating that it is maintained by an internal mechanism rather than continuous sensory or reafferent stimuli.

In principle, the long-duration characteristic of the host-seeking state could be generated by neurons at any point in the circuit. However, it is extensively documented in *Aedes aegypti* that CO_2 sensory neurons show an accurate readout of CO_2 levels over a large concentration range (**Grant et al., 2007, Grant et al., 1995**). These neurons do not show adaptation or prolonged activity (**Grant et al., 1995**) and have similar responses in males and females (**Grant et al., 2007**). While we suspect, based on precedents for persistent states observed in other systems, that the persistent state is controlled in the central brain, we cannot exclude a contribution from the periphery. In mice, circuits originating in the central amygdala promote pursuit and attack during cricket hunting (**Han et al., 2017**), but these behaviors appear time-locked to optogenetic activation and a circuit controlling hunting persistence has not been identified.

Mosquito host seeking shares some characteristics with other social and feeding states (**Asahina et al., 2014, Flavell et al., 2013, Hindmarsh Sten et al., 2021, Marques et al., 2020**). The pursuit of females by males during courtship behavior in *Drosophila* shows especially striking similarities. In response to female sensory cues or stimulation of a subset of *fruitless* neurons, male flies enter a state of increased courtship behaviors and lower thresholds for sensory cues from females (**Clowney et al., 2015, Hindmarsh Sten et al., 2021, Inagaki et al., 2014, Jung et al., 2020**). It appears that this function of *fruitless* is conserved and displays the properties of persistence and sexual dimorphism (**Bertossa et al., 2009, Demir et al., 2005, Manoli et al., 2005**). These similarities suggest that mosquito evolution may have co-opted these properties of ancestral *fruitless* circuits to drive a novel feeding behavior.

This study illuminates why mosquitoes are such effective predators: they maintain the goal of blood feeding for minutes even in the absence of any additional positive stimuli or reinforcement. Because this state greatly outlasts individual sensory stimuli and integrates multiple modalities, any intervention that disrupts this internal drive state should be more effective than vector control measures that mask or disrupt any individual aspect of host-seeking.

Methods

Key Resources Table				
Reagent type (species) or resource	**Designation**	**Source or reference**	**Identifiers**	**Additional information**
recombinant DNA reagent	QUAS-CsChrimson-tdTomato (plasmid)	This study	pTS26, Addgene 175548	Described in Methods section "Creation of CsChrimson mosquitoes for optogenetics"; Available from Addgene
strain, strain background (*Aedes aegypti*)	Liverpool IB12	BEI resources	MRA-735	
genetic reagent (*Aedes aegypti*)	*QUAS-CsChrimson-tdTomato*	This study		Strain available on request from Vosshall or Sorrells labs
genetic reagent (*Aedes aegypti*)	*Gr3-QF2*	doi: https://doi.org/10.1101/2020.11.07.368720		
genetic reagent (*Aedes aegypti*)	*Gr4-QF2*	PMID: 33049200		
antibody	Mouse monoclonal anti-Brp antibody	DSHB	Cat# nc82, RRID:AB_2314866	Immunofluorescence 1:10,000
antibody	Rabbit polyclonal anti-RFP antibody	Rockland	Cat# 600401-379, RRID:AB_2209751	Immunofluorescence 1:1000

antibody	Goat polyclonal anti-mouse Alexa Fluor 647	Thermo Fisher	Cat# A21235, RRID:AB_2535804	Immunofluorescence 1:500
antibody	Goat polyclonal anti-rabbit Alexa Fluor 555	Thermo Fisher	Cat# A32732, RRID:AB_2633281	Immunofluorescence 1:500
software, algorithm	Ctrax	PMID: 19412169		
software, algorithm	JAABA	PMID: 23202433		Downloaded July 15 2020
software, algorithm	APT	https://github.com/kristinbranson/APT		Downloaded July 9 2020

Human and animal ethics statement

Blood feeding of mosquitoes with live anesthetized mice was conducted according to approved institutional animal care and use committee (IACUC) protocol #17108 of The Rockefeller University. Blood feeding of mosquitoes with human volunteers was conducted according to an approved Institutional Review Board (IRB) protocol of The Rockefeller University Hospital under IRB protocol LV-0652. Human volunteers gave written informed consent to participate in the experiments.

Mosquito strains

The following *Aedes aegypti* strains were used in this paper: wild type Liverpool, *Gr3-QF2* (**Younger et al., 2022**), *Gr4-QF2* (**Jové et al., 2020**), fruitless$^{\Delta M}$ (**Basrur et al., 2020**), fruitless$^{\Delta M\text{-tdTomato}}$ (**Basrur et al., 2020**), and *QUAS-CsChrimson* (this study).

Mosquito rearing

Mosquito strains were reared at 26^{o}C ± 2^{o}C with 80% humidity and 14 hours light, 10 hours dark (lights on at 7AM) as previously described (**DeGennaro et al., 2013**). Embryos were hatched in hatching broth: 1 pellet of fish food (TetraMin Tropical Tablets, Pet Mountain 16110M) crushed using a mortar and pestle, added to 850 mL deionized water, then autoclaved. Larvae were reared in deionized water and fed 1-3 tablets of fish food per day. Adult mosquitoes were fed on 10% sucrose (w/v in distilled water) ad libitum. Sucrose was delivered in a Boston clear round 60 mL glass bottle (Fisher FB02911944) filled with 50 mL 10% sucrose. A cotton dental wick (Richmond Dental 201205) was inserted into the bottle and

mosquitoes fed from the sugar-moistened wick. Female mosquitoes were blood fed on mice or human arm to generate eggs. Eggs were dried at 26°C and 80% humidity for 3 days, and then stored at ambient temperature and humidity for up to 3 months. Adults were allowed to mate freely for at least 7 days prior to performing experiments. All behavior experiments were carried out in the light phase of the photoperiod, with most experiments occurring between Zeitgeber (ZT) ZT2 to ZT12.

Creation of CsChrimson mosquitoes for optogenetics

We generated mosquitoes that expressed a translational fusion of CsChrimson to tdTomato under the control of the QUAS promoter, referred to as *CsChrimson* or *QUAS-CsChrimson* throughout the paper. The coding sequence of *CsChrimson-tdTomato* was PCR-amplified from the vector p20X (**Klapoetke et al., 2014**) using the following oligonucleotide primers: forward 5'- CTCGAGCAAAATGAGCAGACTGGTCGCCGCTTC-3', reverse 5'-ATCCTCTAGATTACACCTCGTTCTCGTAGCAGAATTTATACAG-3'. The vector backbone from pXL-BacII-15xQUAS_TATA-SV40 (**Riabinina et al., 2016**) was amplified by PCR using the following oligonucleotide primers: forward 5'-GTCTGCTCATTTTGCTCGAGCCGCGGCCGCAGATC-3', reverse 5'-CGAGGTGTAATCTAGAGGATCTTTGTGAAGGAACCTTACTTCTG-3'. The *CsChrimson* insert was cloned into the backbone using Infusion HD cloning kit (Takara 638920) to create pTS26, available at Addgene (plasmid number 175548). This plasmid was injected into 500 *Aedes aegypti* Liverpool embryos by the Insect Transformation Facility (Rockville, MD) using 200 ng/μL plasmid DNA and 200 ng/μL piggyBac transposase mRNA. Ten independent *QUAS-CsChrimson* integration events were isolated under standard mosquito rearing conditions.

Peripheral sensory appendage microscopy

Mosquitoes 3-4 weeks of age were anesthetized on ice, then maxillary palps and antennae were removed using sharp forceps and placed in fixative (4% paraformaldehyde, 0.1M Millonig's Phosphate Buffer pH 7.4, 0.25% Triton X-100) and nutated for 30 minutes at 4°C. Tissues were washed four times in PBS, then mounted in SlowFade Diamond Antifade Mountant (ThermoFisher). Images were acquired on an Inverted LSM 780 laser scanning confocal microscope (Zeiss) using a 25x 0.8 NA multi-immersion objective with oil. Images were processed using ImageJ.

Brain Immunostaining

Brain immunostaining was carried out as previously described (**Jové et al., 2020**). Mosquitoes 1-2 weeks of age were anesthetized on ice, then heads were removed using forceps and placed into fixative (4% paraformaldehyde, 0.1M Millonig's Phosphate Buffer pH 7.4, 0.25% Triton X-100) and nutated for 3 hours at 4°C. Heads were washed four times in PBS and kept on ice during dissections. The brains were dissected using #5 forceps (Dumont) in a droplet of PBS on a Petri dish coated with SYLGARD silicone elastomer (Dow). Brains were transferred to a 35 μm mesh cap of a flow cytometry test tube (Fisher 08-771-23) in a 24-well plate containing PBSTx (PBS with 0.25% Triton X-100). Brains were washed four times for 30-60 minutes at room temperature in PBSTx on an orbital shaker before permeabilization and between each of the following steps. Brains were permeabilized in PBS with 4% Triton X-100 and 2% normal goat serum for 2 days at 4°C on an orbital shaker. We used the mouse anti-

Bruchpilot (brp) monoclonal antibody at a dilution of 1:10,000. The brp antibody was purified by Frances Weis-Garcia of the Sloan Kettering Institute Antibody & Bioresource from the brp/nc82 hybridoma, developed by Erich Buchner at the Universitätsklinikum Würzburg and obtained from the Developmental Studies Hybridoma Bank, created by the NICHD of the NIH and maintained at The University of Iowa, Department of Biology, Iowa City, IA 52242. Rabbit anti-RFP antibody (Rockland 600-401-379) was used at a dilution of 1:1000 to detect tdTomato fused to CsChrimson as well as the dsRed transgene marker expressed from the *3XP3* enhancer/promoter. Brains were incubated in primary antibodies in PBSTx with 2% normal goat serum for 3 days at 4°C on an orbital shaker. Secondary antibodies were goat anti-mouse Alexa Fluor 647 (Thermo Fisher A21235) and goat anti-rabbit Alexa Fluor 555 (Thermo Fisher A32732) both at 1:500 dilution. Brains were incubated in secondary antibodies in PBSTx and 2% normal goat serum for 2 days at 4°C on an orbital shaker. Brains were washed four more times at room temperature for 30-60 minutes before mounting in SlowFade Diamond Antifade Mountant (ThermoFisher). Images were acquired on an Inverted LSM 880 Airyscan NLO laser scanning confocal microscope (Zeiss) using a 25x 0.8 NA multi-immersion objective with oil. Images were processed using ImageJ.

Rearing mosquitoes for optogenetics

For CsChrimson to respond to red light (625 nm in this paper), it is necessary to supply the all-trans retinal co-factor. Moreover, it is critical that animals reared for optogenetics be maintained in the dark to avoid activating CsChrimson inappropriately. Therefore, we developed a mosquito rearing protocol to deliver all-trans retinal under dark conditions. First, we carried out experiments to select the best *QUAS-CsChrimson* transgenic insertion among the 10 lines we generated. Insertions were identified and tracked using fluorescence from the *3xP3-ECFP* marker. We wanted lines with strong and selective behavioral induction in combination with a QF2 driver, but no basal behavioral activity without a QF2 driver. We also wanted it to be a single insertion at a known position in the genome, that would not obviously disrupt a known gene. The insertion site of the transgene in each line was mapped to the genome using TagMapping (**Stern, 2017**). After being fed with all-trans retinal as described below, all 10 lines were tested for their response to red light with and without being crossed to a QF2 driver. Based on these initial screens, a single line with the *QUAS-CsChrimson* transgene inserted in an intron of the gene LOC23687794 on chromosome 2 at base pair 453,953,698 in the L5.0 version of the *Aedes aegypti* genome (**Matthews et al., 2018**) was selected for use in all subsequent experiments. This *CsChrimson* strain was outcrossed to wild type mosquitoes for 8 generations before being homozygosed and used for behavior experiments. For all experiments except those in Figure 2I,K, which used wild type mosquitoes with a green light startle stimulus, animals were subjected to special rearing conditions to prepare them for optogenetics. Eggs were hatched in 1 L of hatching broth under a 14-hour 450 nm blue light and a 10-hour dark cycle in a light-tight 26°C incubator with 80% humidity. Blue light was selected for the light phase of the photoperiod to avoid activating CsChrimson. The next day 2 L of distilled water was added to the pan, and the following day larvae were thinned to 450 per pan. Larvae were subsequently sorted for fluorescence markers if necessary, using a dissecting microscope. Larvae were fed daily with 1-3 tablets of Tetramin fish food (Pet Mountain 16110M) ground into a powder using a mortar and pestle. Pupae were moved to eclose into adults in a 30 cm x 30 cm x 30 cm insect rearing cage (Bugdorm DP1000) with ad libitum access to 10% sucrose in sugar-feeding glass bottles. Animals were

not sexed at this stage, so cages contained males and females that freely mated. Behavior experiments were performed 1-4 weeks post-pupation. Three days before the experiment, the sugar wicks were replaced with water wicks to starve animals for 24 hours. Two days before the experiment, the water wicks were replaced with wicks soaked in 10% sucrose and 400 μM all-trans retinal (Sigma, R2500-1G). 50 mL of sucrose and all-trans retinal was used per cage. Animals were allowed to feed for 1-3 days in the dark on this meal. In pilot experiments we verified that starved females fed on sucrose and all-trans retinal by observing yellow pigmentation in the abdomen. Feeding in the dark was used to avoid premature neuronal activation and bleaching of the all-trans retinal in the sugar feeders. This rearing protocol was used for all experiments in the opto-membrane feeder, opto-thermocycler, and blood blanket experiments.

Opto-membrane feeder assay

The optomembrane feeder assay was constructed using optomechanical components (Thorlabs MB12, TR12, RA90) and a black 1/4" thick acrylic platform for the canister of mosquitoes to rest on. A hole in the bottom of the platform allowed a camera (Blackfly U3-13S2M-CS, FLIR) outfitted with an 800 nm longpass filter (Midwest Optical LP800-34) to image through the clear canister. Canisters were constructed from a polycarbonate tube of diameter 4.5” (McMaster-Carr 8585K56) and 5” long. The bottom was made of clear 1/8” thick acrylic and attached with plastic epoxy (Loctite 1363118). The top was an inset lid made of black 1/4" and 1/8” inch acrylic and UV-resistant black mesh (McMaster-Carr 87655K13). The canister was surrounded by a coil of RGB LEDs (Digikey 289-1189-ND) spaced 1.5” from the exterior of the canister and controlled by an Arduino Uno board (Arduino A000066). Mosquitoes were illuminated by 850 nm infrared LEDs surrounding the top of the cylinder of RGB LEDs. The assay was enclosed in a black 1/4" thick acrylic box of dimensions 15” x 15” x 28” to prevent ambient light from entering the assay. The top of the acrylic box had an entry port of 4” x 2.7” for CO_2 diffused by a Flystuff Flypad (Genesee Scientific, 59-114), and two doors on the side, one at the level of the cylinder (10” high x 8” wide) and one at the bottom (8” high x 10” wide) at the level of the camera. The day before the experiment, mosquitoes were sexed under cold anaesthesia in white light, placed into the cylindrical canisters, and fed water and 400 μM all-trans retinal in the dark until the experiment commenced. Dental wicks were soaked in approximately 12.5 mL of the water and all-trans retinal, placed on top of the mesh of the inset lid. Trials were run in an environmental room at 25-28^{o}C and 70-80% humidity. For each trial, a canister of 20 mosquitoes was placed on the platform and acclimated for 10 minutes prior to the stimulus. Throughout the acclimation period and trial, the canister was bathed in dim blue 471 nm light from the RGB LEDs. The RGB LEDs were arranged in a coil around the cylindrical canister of mosquitoes to give a relatively even light distribution throughout the canister as measured by a light meter (Coherent Wand UV/VIS Power Sensor 1299161). At the start of the trial, a blood meal consisting of 5 mL of defibrinated sheep blood (Hemostat Laboratories DSB100) with 2 mM ATP (Sigma A6419-1G) heated to 42^{o}C was placed on top of the canister. Blood meals were delivered using an acrylic lid consisting of a 1/16” thick clear acrylic ring with a 2” inner diameter and 2.6” outer diameter attached to a 1/2" thick clear acrylic ring with a 2.3” inner diameter and 2.6” outer diameter. This lid was covered with Parafilm on the 1/16” thick side to create a well for the blood when placed Parafilm-down on the inset lid of the cylindrical canister. At the start of the experiment, the warm blood meal was pipetted onto the Parafilm. On top of the blood meal was an inverted 4 oz bottle (SKS

Bottle & Packaging 0604-07) filled with water heated to 42°C to keep the blood near body temperature for the duration of the 15 minutes trial. Mosquitoes were given CO_2, red light (624 nm, 3.5-6 μW/mm^2), or neither stimulus throughout the 15-minute trial. The light intensity chosen was an intermediate intensity as determined by a light-behavior dose-response curve (Figure 1—figure supplement 1B-D). 10% CO_2 was mixed with filtered room air using flow controllers (Aalborg P26A1-BA2) to deliver a 2.7% CO_2 stimulus through the top of the container. Air flow delivery is described in detail in (**Basrur et al., 2020**). Between trials, the lower door was opened for 5 minutes with the air flow on to flush residual CO_2 from the assay. On a given day of experiments, each of 3 genotypes (*Gr3*, *CsChrimson*, and *Gr3* > *CsChrimson*) was tested with each of the 3 stimuli (no stimulus, CO_2, red light), for a total of 9 trials. The order of trials was rotated between days. Genotypes were blinded to the experimenter. Attraction to the warm blood meal was quantified by manually counting the number of mosquitoes on the warm blood meal in the video (1 frame/second) every 15 seconds. Engorgement was quantified by visual examination of mosquitoes at 4°C after the end of the trial. Between days of experiments, the canisters were cleaned by spraying 70% ethanol with a spray bottle and wiping down with a soft sponge, rinsed with deionized water, and air dried.

Opto-thermocycler assay

The opto-thermocycler assay was constructed on top of a PCR thermocycler (Eppendorf Mastercycler) using optomechanical components (Thorlabs XE25L12, XE25L24, XE25L09, XE25T4, RA90, TRA6, TR12). This assay was used as the basis for experiments delivering light only, light along with heat stimuli, and blood blanket experiments. Light was delivered using six red light 627nm LEDs (Luxeon Star SP-01-D9) or six green light 530nm LEDs (Luxeon Star SP-01-G4) controlled with an Arduino Uno board. Light intensity was measured using a Coherent Wand UV/VIS Power Sensor (1299161) at 9 points on the surface of the PCR block and light angle was adjusted using wires to achieve even illumination. The surface of the PCR block was covered in black tape to reduce glare (Thorlabs T137-2.0). Temperature was measured using a type T thermocouple (Harold G. Schaevitz Industries LLC CPTC-120-X-N) connected to the Arduino board (Arduino A000066) using a thermocouple amplifier (Adafruit MAX31856). The thermocouple sensor was placed on the surface of the lower right of the PCR block and secured using black tape (Thorlabs T137-2.0). Temperature reading and light output were recorded every 100 milliseconds from the Arduino using a custom Processing script. Video was synchronized with the light and temperature stimuli with an infrared 940 nm LED (Adafruit 387) covered with tape and placed in the field of view of the camera. Mosquitoes were illuminated with an infrared 850 nm LED strip (Waveform Lighting 7031.85) surrounding the plate of mosquitoes orthogonal to the view of the camera. Video was recorded using a Blackfly camera (FLIR BFS-U3-16S2M-CS) outfitted with a 780 nm longpass filter (Vision Light Tech LP780-25.5) at 30 frames/second using Spinview software. Heat stimuli were programmed onto the PCR thermocycler to elicit the desired change in temperature from ambient to skin temperature (25-35°C) as measured by the thermocouple (Figure 2B). Red light stimuli were 627 nm at an intensity of 12 μW/mm^2, chosen as an intermediate intensity that allowed the possibility of both an increase and decrease in the behavioral response. Green light stimuli were 530 nm at an intensity of 22 μW/mm^2, chosen because it was the maximum intensity of our setup and to maximize the chance of observing a persistent response to green light. To synchronize the heat and light stimuli, experiments started with a

brief dip in temperature followed by a 10-minute acclimation period after which the experiment started. Experiments in Figure 2E-H were conducted with a single stimulus presented to mosquitoes to determine the duration of response. In all other experiments, mosquitoes received multiple stimuli over the course of a 3–6-hour experiment. Data from the rare trials where the mosquito died during the experiment were discarded. For experiments using red light and heat, trials were delivered 20 minutes apart and the order was pseudorandomized between multiple sweeps of trials and across days. For experiments using green light and heat (Figure 2I,K), the stimuli were pseudorandomized across sweeps only. Sweeps are considered technical replicates conducted on the same individual mosquito, and each mosquito in the assay is a biological replicate. All experiments were conducted multiple times either as a pilot followed by full experiment, or multiple full experiments. Mosquitoes were assayed in a custom acrylic plate with 3 x 5 wells. The sides of the plate were cut using a laser cutter from 1/8" thick clear acrylic, then assembled using acrylic glue (WELD-ON, #4SC Plastic Solvent Glue for Acrylic). The top and bottom were cut from 1/16" acrylic. The top was left removable to load mosquitoes while the bottom was used to sandwich a piece of black fiberglass window screen (Breakthrough Premium Products IHLRS3684BL) creating a mesh bottom for each well. The acrylic bottom piece spaced the mesh bottom of the wells 1.5 mm from the surface of the PCR block. Wells containing the mosquitoes were 18.5 mm long x 17 mm wide x 12 mm high. The well in the lower right was empty to accommodate the thermocouple. The day before the experiment, mosquitoes were sexed under cold anesthesia in white light, placed into the custom plate, and fed water and 400 µM all-trans retinal overnight until the experiment. This was delivered in cotton dental wicks each soaked with 12.5 mL water and all-trans retinal. Three wicks were laid flat beneath each plate so that mosquitoes in all wells could access the wicks beneath. Experiments were run at ambient room temperature and humidity, but the PCR block kept the assay chamber at a fixed temperature. Between trials the surface of the PCR block was cleaned by wiping with a Kimwipe moistened with 70% ethanol. Between days of experiments, the canisters were cleaned by spraying 70% ethanol with a spray bottle and wiping down with a gloved finger, rinsed with deionized water, and air dried.

Blood blanket assay

The opto-thermocycler assay captures probing behavior but does not offer a meal for engorgement. We therefore modified this device to produce the blood blanket assay. The most biologically relevant meal for host-seeking females would be blood, but its opacity makes it unsuitable for our video tracking. We therefore used adenosine 5'-triphosphate (ATP) in saline as a an optically clear proxy for blood. This meal has previously been shown to be highly palatable and triggers mosquito engorgement equivalent to a blood meal (**Galun et al., 1963, Jové et al., 2020**). To modify the opto-thermocycler to accommodate this blood meal substitute, a thin aluminum plate (McMaster-Carr 6061 Aluminum sheet 0.025") was sandwiched between laser cut pieces of acrylic creating wells on the side facing the mosquito. The wells were 18.5 x 17 x 1 mm. The acrylic was bonded to itself using acrylic glue (WELD-ON, #4SC Plastic Solvent Glue for Acrylic) and to the aluminum plate with epoxy (Loctite 1363118) and UV-curing glue (Bondic SK8024). The plate was prepared for a trial by adding 500 µL of the meal (110 mM NaCl, 20 mM $NaHCO_3$, and 2 mM ATP) to each well of the plate in Figure 4A-C. In Figure 4D-F, the composition of the meal was 110 mM NaCl, 10 mM $NaHCO_3$, and 2 mM ATP. The plate was covered with Parafilm to provide a membrane for the mosquitoes to pierce before accessing the meal. The plate was placed directly on top of the

PCR bock to allow maximum heat transfer. The thermocouple was placed on the surface of the Parafilm in the middle of the well in the lower right corner to record the temperature of the heated meal. Trials were carried out and synchronized in the same way as opto-thermocycler experiments. All blood blanket experiments were single trial.

Machine-learning based behavior classification

Videos were pre-processed using a custom Python script tracking_optothermo.py that converted the file format, split up videos into ~30-minute chunks, selected frames to create a background image for centroid tracking, and detected frames where the IR synchronization LED was illuminated. Next, we used Ctrax (**Branson et al., 2009**) for centroid tracking. A background model was created using the selected frames from the experimental video. Ctrax background settings were background brightness high threshold 2.55, low threshold 0.25-0.5 adjusted depending on the video. The area with the infrared synchronization LED was excluded using a region of interest to avoid interference with the tracking. Mosquitoes that moved very little, such that they were visible in the background image, were corrected for using the Fix Background Model option. In tracking settings, shapes were filtered using the following minimum/maximum: 110/1600 for area, 4/36 for major axis, 4/30 for minor axis, 0.0/0.98 for eccentricity. The rest of the tracking settings were default. We used Ctrax centroid tracking as input to Animal Part Tracker (APT, https://github.com/kristinbranson/APT downloaded on July 9, 2020) for tracking points on the mosquito body. For opto-thermocycler experiments we tracked 9 points: the tip and base of the proboscis, the tip of the abdomen, and 3 points on each foreleg: where the femur connects to the body, the join between the femur and the tibia, and the joint between the tibia and the first tarsomere. Tracking the mid legs and hind legs was not needed for behavioral classification so they were excluded to speed computation. Opto-thermocycler classifiers were trained on 320 frames from two videos for female mosquitoes and 102 frames from one video for male mosquitoes. We tracked 13 points for blood blanket experiments, the same 9 points as for opto-thermocycler experiments plus two points at the point of the abdomen where it connects to the thorax and two points at the midpoint or thickest part of the abdomen. The blood blanket classifier was trained on 215 frames from four videos. All APT classifiers were trained using the Cascaded Pose Regression tracking algorithm. Janelia Automatic Animal Behavior Annotator [(JAABA) (**Kabra et al., 2013**), downloaded on July 15 2020] was used for classifying specific behaviors. The classifier for flight (called *fly2*) was used for all videos of females and males. It was trained from two videos and used appearance and locomotion features with radius of 10 frames with no post-processing. The other classifiers additionally used APT information, a larger radius of frames, and minimum bout sizes for improved accuracy. Separate classifiers were trained for females and males in the opto-thermocycler and females in the blood blanket experiments to maximize classifier accuracy in the face of differences in visual appearance. Probing classifiers (*probe5* for female opto-thermocycler experiments, *probemale* for male opto-thermocycler experiments, and *probeBB* for females in the blood blanket experiments) included the pair of points proboscis tip and base as features, along with APT, motion, and appearance features. The grooming and walking classifiers (*walk3* for female and male opto-thermocycler experiments, *groom3* and *groommale* for female and male opto-thermocycler experiments, respectively, and *walkBB* and *groomBB* for blood blanket experiments) were trained using APT, locomotor, and appearance features. APT classifiers were visually inspected for accuracy. APT and JAABA classifiers were evaluated by the accuracy of ground truthing on the JAABA classifiers. An

initial classifier was trained, then ground truthing was performed on 50-100 segments of 1 second video segments that were balanced between segments with and without the behavior. These segments were examined for mis-classified frames and additional training was performed to improve the classifier. Thus, the ground truth dataset is more challenging than a random one because it contains frames that were previously mis-classified and so the real accuracy is higher. Training continued until true positive and true negative rates of were >90% were obtained with 7 of 9 classifiers. Two other classifiers had rates slightly below this. The *groomBB* was trained to ~84% true positive and negative rate because certain grooming postures are difficult to distinguish from probing postures. The *probemale* classifier was trained to ~87% true positive and ~91% true negative rate because only part of the male proboscis is distinguishable from the maxillary palps during probing behavior. Classified behaviors for each mosquito track from JAABA were assigned to single wells according to x-y location of the track to correct the small numbers of frames where Ctrax detected two mosquitoes per well (usually due to a leg that was discontinuous with the rest of the animal) and to connect broken tracks to a single individual mosquito. The IR LED stimulus in the video was aligned with data about temperature and light stimuli from the Arduino and assigned to frames in the video. Velocity was calculated by taking the Ctrax x-y position at 100 ms intervals (3 frames).

Analysis of behavior

To calculate the half-life of the mosquito behavior response in Figure 2H-J and Figure 3C,H, the baseline was calculated as the average probing in 2 minutes prior to stimulus onset. A sliding window of the amount of probing was calculated in 15 second windows starting at stimulus onset for every frame. The maximum response was defined as the window with the greatest probing after stimulus onset and $t_{1/2}$ was defined as the first window in which the probing was halfway between the maximum response and the baseline. To calculate the integration of heat and the second stimuli (fictive CO_2, fictive sugar, or green light) in Figure 2—figure supplement 2 and Figure 2M, we calculated the average response to each of the individual stimuli. We added the two responses to get a predicted additive response. For each individual mosquito, we divided its response by the predicted additive response and multiplied by 100%. This gave a percent additivity where 0% was no response and 100% was exactly additive. For line graphs, the additivity signal was smoothed over 4.5 seconds around each 500-millisecond timepoint.

tSNE analysis

To infer the state of individual mosquitoes in the blood blanket experiment, we split each mosquito track into 30 second intervals at 10 second step size and calculated 38 parameters. The 30 second time interval was selected as a period of time over which the behaviors exhibited were relevant to interpreting the internal state of the mosquito. The time interval was varied from 10 to 60 seconds to assure that the results were not sensitive to this parameter choice (Figure 4—figure supplement 2). The parameters included the proportion of the time window that mosquitoes exhibited each behavior and no behavior. Mosquitoes can probe and walk at the same time so the proportion of time probing and walking, probing not walking, and walking not probing were included. The number of bouts of each behavior was included. Velocity parameters included average velocity over the window and average velocity during each behavior. Transitions between behaviors were included as outgoing rate per second of transition to all other behaviors or no behavior. For the purposes of transitions and ethograms,

probing and walking were treated as mutually exclusive with probing taking higher precedence over walking. For all behaviors to avoid rare frames where multiple behaviors were classified for a single frame the precedence of behaviors were flying > probing > walking > grooming > no behavior. Based on the total amount of time animals spent performing each behavior, cutoffs were determined to specify a minimum amount of behavior exhibited. Cutoffs were 0.04 for flight, 0.2 for walking or probing, and 0.3 for grooming. Behavior below these cutoffs was excluded from further analysis. The Python package scikit-learn (https://scikit-learn.org/ version 0.24.1) was used for tSNE embedding with parameters n/100 perplexity (1061), and other default parameters (200 learning rate, 1000 iterations). Multiple perplexities were compared to assure that results were not sensitive to this parameter choice. tSNE plots were examined and clusters were segmented manually by grouping densely clustered points. These clusters were used to annotate videos for visual inspection of what mosquito behaviors they corresponded to. Names for clusters were chosen based on the characteristics of the clusters shown in Figure 4K, Figure 4—figure supplement 1B, Figure 4—figure supplement 2, and video observation. Clusters that included mosquitoes that moved around were named Global or Local search based on the total amount of movement and contrasting amounts of flight and walk behaviors. The cluster that included mostly grooming was termed Rest. The cluster that included mosquitoes that were stationary, probing, and with abdomens expanded after feeding was termed Engorge. The clusters for Rest, Global Search, and Local Search were single clusters that were clearly differentiated on the tSNE embedding. The Engorge cluster was composed of two smaller clusters that, when observed on video, both consisted of mosquitoes engorging and were therefore combined. Points on the end of the Local Search cluster in the tSNE embedding with high probing were also examined by video and grouping was kept with the Local Search cluster.

Statistical analyses

R (https://www.r-project.org version 4.0.5) and Python were used for statistical analysis. Data distributions were visually examined for normality or tested using the Shapiro-Wilk test. Normally distributed samples were compared by one sample t-test for paired measurements or ANOVA and Tukey's test for multiple categories. Non-normally distributed samples were compared using the Friedman test for multiple category repeated measurements, Kruskal-Wallis test for multiple category single measurements, or the sign test for skewed paired measurements. The Friedman and Kruskal-Wallis test were used with Nemenyi post-hoc tests to determine pairwise differences between categories. T-tests and sign tests were adjusted using Holm's method for correcting for multiple comparisons. For statistical analyses involving comparisons of the behavior of males and females, we repeated the tests after accounting for differences in classifier accuracy by changing the proportion of behavior by this difference (i.e. 4.93% for probing and 3.25% for walking) and confirming that the results were the same. Sample sizes followed conventions in the field. For experiments with multiple stimuli presented to each animal, 4-6 days of data were collected. For endpoint and single stimulus experiments, 7-11 days of data were collected.

Logistic Regression

Logistic regression models for the blood blanket experiment were trained using the Python sklearn package with the proportion of time mosquitoes spent in each of the four behaviors (groom, walk, probe, and fly) for two minutes after the light stimulus as predictors. These

periods of time were -2 to 0 minutes, -8 to -6 minutes, and -14 to -12 minutes relative to the heat stimulus for the 2-minute, 8-minute, and 14-minute inter stimulus interval experiments. The dependent variable was whether the mosquito engorged by the end of the experiment. Models used the liblinear solver, random_state of 0, and balanced weight_class. Bootstrapping was performed using 10,000 resamples with replacement of the engorgement dataset to determine the distribution of predictive models. 10,000 shuffles of the engorgement data were used to determine whether the predictive model performed above chance. Leave-one-out cross-validation was used to determine whether the model was overfitted.

Data availability

All data generated or analyzed during this study are included in the manuscript and in Figure 1 – source data 1, Figure 2 - source data 1, Figure 3 – source data 1, and Figure 4 – source data 1. Large datasets are available at https://github.com/trevorsorrells/Optothermocycler.

Code availability

Analysis code used in this publication is available at https://github.com/trevorsorrells/Optothermocycler.

References

Álvarez-Salvado E, Licata AM, Connor EG, McHugh MK, King BM, Stavropoulos N, Victor JD, Crimaldi JP, Nagel KI. 2018. Elementary sensory-motor transformations underlying olfactory navigation in walking fruit-flies. *Elife* **7**: e37815.

Anholt BR, Ludwig D, Rasmussen JB. 1987. Optimal pursuit times: How long should predators pursue their prey? *Theor Popul Biol* **31**: 453-464

Araripe LO, Bezerra JRA, Rivas G, Bruno RV. 2018. Locomotor activity in males of *Aedes aegypti* can shift in response to females' presence. *Parasit Vectors* **11**: 254

Asahina K, Watanabe K, Duistermars BJ, Hoopfer E, Gonzalez CR, Eyjolfsdottir EA, Perona P, Anderson DJ. 2014. Tachykinin-expressing neurons control male-specific aggressive arousal in *Drosophila*. *Cell* **156**: 221-235

Basrur NS, De Obaldia ME, Morita T, Herre M, von Heynitz RK, Tsitohay YN, Vosshall LB. 2020. *Fruitless* mutant male mosquitoes gain attraction to human odor. *Elife* **9**: e63982

Bertossa RC, van de Zande L, Beukeboom LW. 2009. The *fruitless* gene in *Nasonia* displays complex sex-specific splicing and contains new zinc finger domains. *Mol Biol Evol* **26**: 1557-1569

Branson K, Robie AA, Bender J, Perona P, Dickinson MH. 2009. High-throughput ethomics in large groups of *Drosophila*. *Nat Methods* **6**: 451-457

Chari T, Banerjee J, Pachter L. 2021. The specious art of single-cell genomics. *bioRxiv*: DOI 10.1101/2021.1108.1125.457696

Clowney EJ, Iguchi S, Bussell JJ, Scheer E, Ruta V. 2015. Multimodal chemosensory circuits controlling male courtship in *Drosophila*. *Neuron* **87**: 1036-1049

Corfas RA, Vosshall LB. 2015. The cation channel TRPA1 tunes mosquito thermotaxis to host temperatures. *Elife* **4**: e11750

DeGennaro M, McBride CS, Seeholzer L, Nakagawa T, Dennis EJ, Goldman C, Jasinskiene N, James AA, Vosshall LB. 2013. *orco* mutant mosquitoes lose strong preference for humans and are not repelled by volatile DEET. *Nature* **498**: 487-491

Dekker T, Carde RT. 2011. Moment-to-moment flight manoeuvres of the female yellow fever mosquito (*Aedes aegypti* L.) in response to plumes of carbon dioxide and human skin odour. *J Exp Biol* **214**: 3480-3494

Dekker T, Geier M, Carde RT. 2005. Carbon dioxide instantly sensitizes female yellow fever mosquitoes to human skin odours. *J Exp Biol* **208**: 2963-2972

Demir E, Dickson BJ. 2005. *fruitless* splicing specifies male courtship behavior in *Drosophila*. *Cell* **121**: 785-794

Demir M, Kadakia N, Anderson HD, Clark DA, Emonet T. 2020. Walking *Drosophila* navigate complex plumes using stochastic decisions biased by the timing of odor encounters. *Elife* **9**: e57524

Duvall LB, Basrur NS, Molina H, McMeniman CJ, Vosshall LB. 2017. A peptide signaling system that rapidly enforces paternity in the *Aedes aegypti* mosquito. *Curr Biol* **27**: 3734-3742

Eiras AE, Jepson PC. 1991. Host location by *Aedes aegypti* (Diptera: Culicidae): a wind tunnel study of chemical cues. *B Entomol Res* **81**: 151-160

Endler JA. 1991. Interactions between predators and prey. In *Behavioral Ecology*, Krebs JR, Davies NB (eds) pp 169-196. Oxford, UK: Blackwell

Flavell SW, Pokala N, Macosko EZ, Albrecht DR, Larsch J, Bargmann CI. 2013. Serotonin and the neuropeptide PDF initiate and extend opposing behavioral states in *C. elegans*. *Cell* **154**: 1023-1035

Galun R, Avi-Dor Y, Bar-Zeev M. 1963. Feeding response in *Aedes aegypti*: Stimulation by adenosine triphosphate. *Science* **142**: 1674-1675

Geier M, Bosch OJ, Boeckh J. 1999. Influence of odour plume structure on upwind flight of mosquitoes towards hosts. *J Exp Biol* **202**: 1639-1648

Grant AJ, O'Connell RJ. 2007. Age-related changes in female mosquito carbon dioxide detection. *J Med Entomol* **44**: 617-623

Grant AJ, Wigton BE, Aghajanian JG, O'Connell RJ. 1995. Electrophysiological responses of receptor neurons in mosquito maxillary palp sensilla to carbon dioxide. *J Comp Physiol [A]* **177**: 389-396

Han W, Tellez LA, Rangel MJ, Jr., Motta SC, Zhang X, Perez IO, Canteras NS, Shammah-Lagnado SJ, van den Pol AN, de Araujo IE. 2017. Integrated control of predatory hunting by the central nucleus of the amygdala. *Cell* **168**: 311-324

Hartberg WK. 1971. Observations on the mating behaviour of *Aedes aegypti* in nature. *Bull World Health Organ* **45**: 847–850

Hindmarsh Sten T, Li R, Otopalik A, Ruta V. 2021. Sexual arousal gates visual processing during *Drosophila* courtship. *Nature* **595**: 549-553

Inagaki HK, Jung Y, Hoopfer ED, Wong AM, Mishra N, Lin JY, Tsien RY, Anderson DJ. 2014. Optogenetic control of *Drosophila* using a red-shifted channelrhodopsin reveals experience-dependent influences on courtship. *Nat Methods* **11**: 325-332

Jové V, Gong Z, Hol FJH, Zhao Z, Sorrells TR, Carroll TS, Prakash M, McBride CS, Vosshall LB. 2020. Sensory discrimination of blood and floral nectar by *Aedes aegypti* mosquitoes. *Neuron* **108**: 1163–1180

839 Jung Y, Kennedy A, Chiu H, Mohammad F, Claridge-Chang A, Anderson DJ. 2020. Neurons
840 that function within an integrator to promote a persistent behavioral state in *Drosophila*. *Neuron*
841 **105**: 322-333

842 Kabra M, Robie AA, Rivera-Alba M, Branson S, Branson K. 2013. JAABA: interactive machine
843 learning for automatic annotation of animal behavior. *Nat Methods* **10**: 64-67

844 Kadakia N, Demir M, Michaelis BT, Reidenbach MA, Clark DA, Emonet T. 2021. Odor motion
845 sensing enables complex plume navigation. *bioRxiv* **10.1101/2021.09.29.462473**

846 Klapoetke NC, Murata Y, Kim SS, Pulver SR, Birdsey-Benson A, Cho YK, Morimoto TK,
847 Chuong AS, Carpenter EJ, Tian Z, Wang J, Xie Y, Yan Z, Zhang Y, Chow BY, Surek B,
848 Melkonian M, Jayaraman V, Constantine-Paton M, Wong GK et al. 2014. Independent optical
849 excitation of distinct neural populations. *Nat Methods* **11**: 338-346

850 Klowden M. 1981. Initiation and termination of host-seeking inhibition in *Aedes aegypti* during
851 oöcyte maturation. *J Insect Physiol* **27**: 799-803

852 Koehl MA. 2006. The fluid mechanics of arthropod sniffing in turbulent odor plumes. *Chem*
853 *Senses* **31**: 93-105

854 Körding K. 2007. Decision theory: what "should" the nervous system do? *Science* **318**: 606-
855 610

856 Lafferty KD, Kuris AM. 2002. Trophic strategies, animal diversity and body size. *Trends Ecol*
857 *Evol* **17**: 507-513

858 Lahondere C, Vinauger C, Okubo RP, Wolff GH, Chan JK, Akbari OS, Riffell JA. 2020. The
859 olfactory basis of orchid pollination by mosquitoes. *Proc Natl Acad Sci U S A* **117**: 708-716

860 Liu MZ, Vosshall LB. 2019. General visual and contingent thermal cues interact to elicit
861 attraction in female *Aedes aegypti* mosquitoes. *Curr Biol* **29**: 2250-2257 e2254

862 Manoli DS, Foss M, Villella A, Taylor BJ, Hall JC, Baker BS. 2005. Male-specific *fruitless*
863 specifies the neural substrates of *Drosophila* courtship behaviour. *Nature* **436**: 395-400

864 Marques JC, Li M, Schaak D, Robson DN, Li JM. 2020. Internal state dynamics shape
865 brainwide activity and foraging behaviour. *Nature* **577**: 239-243

866 Matthews BJ, Dudchenko O, Kingan SB, Koren S, Antoshechkin I, Crawford JE, Glassford WJ,
867 Herre M, Redmond SN, Rose NH, Weedall GD, Wu Y, Batra SS, Brito-Sierra CA, Buckingham
868 SD, Campbell CL, Chan S, Cox E, Evans BR, Fansiri T et al. 2018. Improved reference
869 genome of *Aedes aegypti* informs arbovirus vector control. *Nature* **563**: 501-507

870 Matthews BJ, McBride CS, DeGennaro M, Despo O, Vosshall LB. 2016. The
871 neurotranscriptome of the *Aedes aegypti* mosquito. *BMC Genomics* **17**: 32

McMeniman CJ, Corfas RA, Matthews BJ, Ritchie SA, Vosshall LB. 2014. Multimodal integration of carbon dioxide and other sensory cues drives mosquito attraction to humans. *Cell* **156**: 1060-1071

Pang R, van Breugel F, Dickinson M, Riffell JA, Fairhall A. 2018. History dependence in insect flight decisions during odor tracking. *PLoS Comput Biol* **14**: e1005969

Potter CJ, Tasic B, Russler EV, Liang L, Luo L. 2010. The Q system: a repressible binary system for transgene expression, lineage tracing, and mosaic analysis. *Cell* **141**: 536-548

Riabinina O, Task D, Marr E, Lin CC, Alford R, O'Brochta DA, Potter CJ. 2016. Organization of olfactory centres in the malaria mosquito *Anopheles gambiae*. *Nat Commun* **7**: 13010

Rudolfs W. 1922. Chemotropism of mosquitoes. *New Jers AES Bull* **367**: 5-23

San Alberto DA, Rusch C, Zhan Y, Straw AD, Montell C, Riffell JA. 2021. The olfactory gating of visual preferences to human skin and colors in mosquitoes. *bioRxiv*: 10.1101/2021.1107.1126.453916

Stern DL. 2017. Tagmentation-based mapping (TagMap) of mobile DNA genomic insertion sites. *bioRxiv*: DOI: 10.1101/037762

Suver MP, Matheson AMM, Sarkar S, Damiata M, Schoppik D, Nagel KI. 2019. Encoding of wind direction by central neurons in *Drosophila*. *Neuron* **102**: 828-842.e827

van Breugel F, Riffell J, Fairhall A, Dickinson MH. 2015. Mosquitoes use vision to associate odor plumes with thermal targets. *Curr Biol* **25**: 2123-2139

Vergassola M, Villermaux E, Shraiman BI. 2007. 'Infotaxis' as a strategy for searching without gradients. *Nature* **445**: 406-409

Williams TM, Wolfe L, Davis T, Kendall T, Richter B, Wang Y, Bryce C, Elkaim GH, Wilmers CC. 2014. Mammalian energetics. Instantaneous energetics of puma kills reveal advantage of felid sneak attacks. *Science* **346**: 81-85

Younger MA, Herre M, Ehrlich AR, Gong ZY, Gilbert ZN, Rahiel S, Matthews BJ, Vosshall LB. 2020. Non-canonical odor coding ensures unbreakable mosquito attraction to humans. *bioRxiv* **10.1101/2020.11.07.368720v1**

Younger MA, Herre M, Goldman OV, Lu T-C, Caballero-Vidal G, Qi Y, Gilbert ZN, Gong Z, Morita T, Rahiel S, Ghaninia M, Ignell R, Matthews BJ, Li H, Vosshall LB. 2022. Non-canonical odor coding in the mosquito. *bioRxiv* **10.1101/2020.11.07.368720v2**

Acknowledgements

We thank Hessam Akhlaghpour, Josie Clowney, Emily Dennis, Ann Kennedy, Philip Kidd, and members of the Vosshall lab for comments on the manuscript. We thank Allen Lee, Alice Robie, and Kristin Branson for sharing their unpublished Animal Part Tracker and providing technical help with running it. We thank Jason Banfelder and Rebecca Bennett with software setup on the Rockefeller High Performance Computing Cluster; Jim Petrillo, Dan Gross, and Peer Strogies at the Rockefeller Precision Instrumentation Technologies facility for assistance with design and fabrication of behavior assays; Gloria Gordon and Libby Mejia for expert mosquito rearing; Tom Hindmarsh Sten, Veronica Jové, Gaby Maimon, Ben Matthews Chris Potter, Vanessa Ruta, and Nilay Yapici for discussions; Annie Handler, Jazz Weisman, and Ari Zolin for technical advice with optogenetics experiments; Ben Matthews, Meg Younger, and the Aedes Toolkit Group for access to unpublished strains; Cong Li for assisting with an early version of the individual state analysis; and Rob Harrell at the Insect Transformation Facility for embryo injections. Pilot experiments for this study used an optogenetic setup in the lab of Vanessa Ruta. This work was funded by a Jane Coffin Childs postdoctoral Fellowship (T.R.S.), and a Kavli Neural Systems Institute Pilot Grant and Postdoctoral Fellowship (T.R.S.). L.B.V. is an investigator of the Howard Hughes Medical Institute.

Competing interests

The authors declare no competing interests.

Materials & Correspondence

Correspondence and materials requests should be addressed to Trevor Sorrells and Leslie Vosshall.

Supplementary figures and tables

Figure 1—figure supplement 1, Figure 2—figure supplements 1 and 2, Figure 3—figure supplement 1, Figure 4—figure supplements 1 and 2, and Video 1 accompany the paper.

Supplementary information

Figure 1 – source data 1, Figure 2 – source data 1, Figure 3 – source data 1, and Figure 4 – source data 1 include information on the accuracy of the behavioral classifier and all raw data and statistical analysis in the paper, including sample sizes, exact p-values, and tests performed.

Figure 1. Optogenetic control of mosquito host seeking and blood feeding. (**A**) Schematic of human host cues experienced by a host-seeking mosquito over time. (**B**) Schematic of genetic reagents used for optogenetic activation of CO_2-sensitive *Gr3* sensory neurons. (**C**) Female *Aedes aegypti*, grey boxes indicating antenna (top) and maxillary palp (bottom). Photo: Alex Wild. (**D**) Intrinsic tdTomato fluorescence of whole mounted *Gr3 > CsChrimson* female mosquito antenna and maxillary palp. Scale bar: 50 µm. (**E**) Maximum-intensity projections of confocal Z-stacks of antennal lobes in the right-brain hemisphere of the indicated genotype with immunofluorescent labelling of tdTomato (red) and the synaptic marker BRP (grayscale). Scale bar: 10 µm. (**F**,**G**) Diagram **F** and stimulus protocol **G** of optogenetic behavior assay for mosquito movement. (**H**) Time maximum projection of a single mosquito in the assay in **F** for 30 seconds pre- (left) and post- (right) stimulus. Scale bar: 0.5 cm. (**I**) Velocity of individual mosquitoes of the indicated genotypes 30 seconds pre- and post-stimulus onset. Data are plotted as mean of individual mosquitoes (thin grey lines) with median across individuals indicated with thick black or red line (*$P < 0.0001$, Wilcoxon signed rank test with Holm's correction for multiple comparison, n.s., not significant, n=70 mosquitoes/genotype). (**J**) Schematic of opto-membrane feeder (top) and stimulus protocol (bottom). (**K**) Still images of mosquitoes of the indicated genotype underneath the warm blood meal approximately 7 minutes after the start of red-light stimulation. Scale bar: 1 cm. (**L**) Occupancy of mosquitoes on warm blood meal in the opto-membrane feeder. Data are plotted as mean (line) ± S.E.M. (shading). Data labelled with different letters are significantly different at the 5-minute timepoint ($P < 0.05$, Kruskal-Wallis test followed by Nemenyi post-hoc tests; n=6-7 trials per genotype/stimulus combination, 18-21 mosquitoes/trial). (**M**) Percent of mosquitoes visually scored as engorged at the conclusion of the experiment in **L**. Data are plotted as dot-box plots (median: horizontal line, interquartile range: box, 1.5 times interquartile range: whiskers. Data labelled with different letters are significantly different ($P < 0.05$, Kruskal-Wallis test followed by Nemenyi post-hoc tests; n=7 trials per genotype/stimulus combination and 18-21 mosquitoes/trial). See also Figure 1—figure supplement 1 and Figure 1—source data 1.

Figure 2. Fictive CO_2 induces a persistent behavior state. (**A,B**) Schematic of opto-thermocycler assay **A** and stimuli delivered **B**. (**C**) Still image of a mosquito with pose tracking of 9 points using Animal Part Tracker. Scale bar: 0.5 cm. (**D**) Still images of a mosquito exhibiting the indicated classified behaviors (top). Representative plot of proboscis length with classified behavior superimposed (bottom). Scale bar: 0.5 cm. (**E**) Ethograms of individual mosquitoes of the indicated genotypes. Data show 1 minute before and an excerpt of the 2 minute after the indicated stimuli from a 20 minute experiment. Each row represents data from one mosquito. The experiment comprised a total of n=68-70 mosquitoes/condition. All data were sorted by probing, and every third mosquito (n=22-23) was selected for display here for clarity. (**F,G**) Quantification of walking **F** and probing **G** behavior exhibited by individual mosquitoes from the experiment in **E** during the 5 minute after stimulus onset. Data are plotted as violin-box plots (median: horizontal line, interquartile range: box, 5^{th} and 95^{th} percentiles indicated: whiskers). Data labelled with different letters are significantly different ($P<0.05$, Kruskal-Wallis test followed by Nemenyi post-hoc tests, n.s., not significant, n=68-70 mosquitoes/genotype, 1 stimulus per trial). (**H**) Plot of percent individual *Gr3 > CsChrimson* mosquitoes exhibiting the indicated behavior from 2 minute before to 15 minutes after stimulus onset. Data from experiment in **E**. (**I,J**) Plot of percent individual wild type **I** and *Gr4 > CsChrimson* **J** mosquitoes exhibiting the indicated behavior from 1 minute before to 2 minutes

after stimulus onset **I** or 2 minutes before to 15 minutes after stimulus onset **J** excerpted from a 20 minute experiment. (**I**: n=140 mosquitoes, average of 2 stimulus presentations/mosquito; **J**: n=69 mosquitoes, average of 3 stimulus presentations/mosquito). Flower image used for *Gr4 > CsChrimson* indicates that plant nectar is a sugar source. (**K,L**) Quantification of **I** and **J** for 5 minutes after stimulus onset. Data are plotted as violin-box plots (median: horizontal line, interquartile range: box, 5^{th} and 95^{th} percentiles: whiskers). Distribution represents individual mosquitoes, averaged over multiple stimulus presentations. Data labelled with different letters are significantly different (P<0.05, Friedman test followed by Nemenyi post-hoc tests, n.s., not significant). (**M**) Median additivity of heat and the indicated stimuli presented simultaneously. Additivity of 100% corresponds to the) case when combined stimuli equal the sum of responses to individual stimuli. Data from **E-L**. See also Figure 2—figure supplement 1, Figure 2—figure supplement 2, and Figure 2—source data 1.

Figure 3. The persistent state is specific to host seeking. (**A-C**) Response of non-blood-fed female **A**, blood-fed female **B**, and male **C** *Gr3 > CsChrimson* mosquitoes to the indicated stimuli, plotting each behavior from 2 minutes before to 15 minutes after stimulus onset (n=98/group, average of 3 stimulus presentations/mosquito). (**D,E**) Quantification of walking **D** and probing **E** from data in **A-C** for 5 minutes after stimulus onset. (**F-H**) The behavioral response of males of the indicated genotype for 15 minutes after the indicated stimuli, plotting each behavior from 2 minutes before to 15 minutes after stimulus onset (n=97-98/genotype, average of 3 stimulus presentations/mosquito). (**I,J**) Quantification of walking **I** and probing **J** from data in **F-H** for 5 minutes after stimulus onset. In **D,E** and **I,J**, data are plotted as violin-box plots (median: horizontal line, interquartile range: box, 5th and 95th percentiles: whiskers). The distribution represents individual mosquitoes, averaged over multiple stimulus presentations. Data labelled with different letters are significantly different (P<0.05, Kruskal-Wallis test followed by Nemenyi post-hoc tests, n.s., not significant). See also Figure 3—figure supplement 1 and Figure 3—source data 1.

Figure 4. The persistent state integrates host cues and decision making in time. (**A-F**) Schematic of stimuli presentation **A,D** and quantification of walking **B,E** and probing **C,E** in the 5 minutes after the first stimulus onset (n=111-112 mosquitoes, 2 stimulus presentations/mosquito). In **B**, **C**, **E**, and **F**, data are displayed as violin-box plots (median: horizontal line, interquartile range: box, 5th and 95th percentiles: whiskers). Data labelled with different letters are significantly different (P<0.05, Friedman test followed by Nemenyi post-hoc tests). Data that are significantly different from heat or light are shaded in brown **B**,**E** or red **C**,**F**. (**G**) Schematic of blood blanket assay which uses a blood meal mimic. (**H**) Still images of unfed (top) and fed (bottom) mosquitoes. Scale bar: 1 mm. (**I**) Percent mosquitoes engorged in response to the indicated stimuli in the blood blanket assay (n=9 trials/stimulus, 14 mosquitoes/trial). Data labelled with different letters are significantly different (P<0.05, ANOVA followed by Tukey's post-hoc test). (**J**) Percent mosquitoes engorged in response to the indicated cues in the blood blanket assay (14 mosquitoes/trial n=11 trials/stimulus). Data in **I,J** are displayed as dot-box plots (median: horizontal line, interquartile range: box, 1.5 times interquartile range: whiskers). Dot-box plots in **J** with a red border signify data where combined light and heat stimuli are greater than the sum of individual stimuli (*P<0.05, Student's t-test, after adjustment for multiple comparisons using Holm's method). (**K**) Transition ethograms for each of the four states indicating the proportion of each behavior and the rate of transitions

between them, with dashed rectangle highlighting difference between global and local search. (**L**) Inferred states of 168 individual mosquitoes from the 2 minutes pre-heat stimulus from experiment in **J**, separated into those that were visually scored as unfed (top, n=108) or fed (bottom, n=60) at the end of the experiment. Each row represents data from one mosquito and data are sorted according to the amount of local search during the pre-heat period. White indicates none of the four states were inferred (i.e. the mosquito was primarily motionless). (**M**) Quantification of the percent of time mosquitoes spent in the indicated state during the 2 minutes pre-heat period. Data are plotted as violin-box plots (median: horizontal line, interquartile range: box, 5th and 95th percentiles: whiskers (*P< 0.01, Mann-Whitney U-test, n.s., not significant). (**N**) Performance of a classifier trained on the proportion of each behavior in pre-heat period and used to predict feeding (magenta arrow) along with 10,000 bootstrapped classifiers (magenta violin plot). Chance value (cyan arrowhead) indicates the median performance of model on 10,000 shuffles (cyan violin plot) of the feeding data in **J**. (n=166-168 mosquitoes/stimulus, P=2e-4, 0.0246, 0.0123 for 2, 8, and 14 minutes pre-heat periods, respectively, bootstrapped z-test). (**O**) Summary of the persistent internal state for host-seeking behavior. Color of the mosquito silhouettes indicates the behavior depicted using the colors in **K**. See also Figure 4—figure supplement 1, Figure 4—figure supplement 2, and Figure 4—source data 1.

Figure 1—figure supplement 1. Validation of optogenetic tools. (**A**) Maximum-intensity projections of confocal Z-stacks of whole brains of the indicated genotype with immunofluorescent labelling with an anti-RFP antibody that recognizes both dsRed (indicating expression of the *3xP3-dsRed* transgene marker) and tdTomato (indicating CsChrimson) in red and the synaptic marker BRP in grayscale. The *3XP3* enhancer expresses extensively in the visual system as well as in scattered cells in the brain. Because of spectral overlap, it is not possible to separate the expression of *3XP3-dsRed* and *Gr3>CsChrimson:tdTomato* in this preparation. However, previously published work using a GFP as a marker expressed in *Gr3-QF2* animals allowed us to establish the specificity of *Gr3-QF2* expression to a subpopulation of maxillary palp neurons that project to a single antennal lobe glomerulus (**Younger et al., 2022**). Note the absence of red fluorescence in the middle panel because this transgene is marked by *3XP3-ECFP*. Scale bar: 50 μm. **B**) Response of *Gr3 > CsChrimson* mosquitoes to 5-second stimuli of the indicated light intensities, from 2 minutes before to 15 minutes after stimulus onset (n=98, average of 3 stimulus presentations/mosquito). $t_{1/2}$ indicates the time for walking behavior to return half-way back to baseline. (**C,D**) Quantification of walking **C** and probing **D** from data in **B** for 5 minutes after stimulus onset. (P<0.05, Friedman test followed by Nemenyi post-hoc tests).

Figure 2—figure supplement 1. Fictive CO_2 triggers flight events for 15 minutes. (**A,C**) Percent indicated behavior of *Gr3 > CsChrimson* females from 2 minutes before to 15 minutes after stimulus onset in response to the indicated stimuli. Data from Figure 2E-H. (**B,D**) Quantification of the behavior in **A**, **C** along with data collected from the additional indicated genotypes. Data from Figure 2E-H. Data are plotted as violin-box plots (median: horizontal line, interquartile range: box, 5th and 95th percentiles: whiskers). Data labelled with different letters are significantly different (P<0.05, Kruskal-Wallis test followed by Nemenyi post-hoc tests. n.s., not significant, n=68-70 mosquitoes).

Figure 2—figure supplement 2. Host cues are integrated with different computations than non-host cues. (**A**) Mosquitoes sense host cues separately and simultaneously at different distances from the host. (**B-D**) Responses to individual **B** or combined **C** stimuli or a computed sum of individual stimuli **D**. Plots in **B,C** are reprinted from Figure 2H for comparison with **D**. (**E**) Differences between calculated and actual responses for the indicated genotypes and stimuli from 30 seconds before to 1 minute after stimulus onset, smoothed using a box filter of radius 2.25 seconds. n=70 for *Gr3 > CsChrimson*, n=69 for *Gr4 > CsChrimson*, n=140 for wild type. (**F**) Quantification of E for the first 15 seconds after stimulus onset. Data are plotted as violin-box plots (median: horizontal line, interquartile range: box, 5th and 95th percentiles: whiskers. (**P*<0.0001, sign test using Holm's correction for multiple comparisons, n.s., not significant).

Figure 3—figure supplement 1. Blood-fed mosquitoes respond to fictive sugar. (**A**) Response of blood-fed female *Gr3 > CsChrimson* mosquitoes to the indicated stimuli, plotting each behavior from 2 minutes before to 15 minutes after stimulus onset (n=69/group, average of 3 stimulus presentations/mosquito). (**B-E**) Quantification of change in probing from one minute prior to stimulus onset to one minute after. Data in **B** are from Figure 2J, data in **C** are from **A**, and data in **D-E** are from Figure 3A and 3B. Data are plotted as violin-box plots (median: horizontal line, interquartile range: box, 5th and 95th percentiles: whiskers. (**P*<0.05, Wilcoxon one sample test with Holm's correction for multiple comparisons).

Figure 4—figure supplement 1. Inference of internal state from behavior. (**A**) Schematic of analysis. Classified behavior reflects the output of APT followed by JAABA behavior classifiers. (**B**) t-stochastic neighbor embedding (tSNE) for 30 second time windows spanning 4 minutes prior to the light stimulus to 10 minutes after heat onset for individual mosquitoes from Figure 4J. Points are colored by strong enrichment of the corresponding behavior. State categories were bounded with a black line by visual inspection of the tSNE plot, graphing the behavior characteristics of each cluster, and comparing with video of the mosquitoes in each state. Shown is a random subset of 3,000 time windows from 106,076 total windows from all 7 stimulus types, n=1,162 mosquitoes. (**C**) Total distance travelled over the course of 30 second time windows for each behavior state with the following number windows from each state: engorge, n=5,634; local search, n=11,124; global search, n=15,466; rest, n=9,891. Time windows were taken from 4 minutes before the light stimulus to 10 minutes after heat onset. Data are plotted as violin-box plots (median: horizontal line, interquartile range: box, 5th and 95th percentiles: whiskers). Data labelled with different letters are significantly different (*P*< 0.0001, Kruskal-Wallis test followed by Nemenyi post-hoc tests).

Figure 4—figure supplement 2. Mosquito states are consistent across window duration. (**A-D**) tSNE for time windows of the indicated duration for individual mosquitoes from Figure 4J. Points are colored by strong enrichment of the corresponding behavior. State categories were bounded with a black line by visual inspection of the tSNE plot. Shown is a random subset of 3,000 time windows from 103,658 **A**, 105,387 **B**, 106,044 **C**, and 105,287 **D** total windows from all 7 stimulus types, n=1,162 mosquitoes.

Video 1. Mosquito response to fictive CO_2. Shown is video of the opto-thermocycler assay of female *Gr3 > CsChrimson* mosquitoes responding to a 5-second pulse of red light. Points

tracked on the body of the mosquito are indicated by white semi-transparent dots and behaviors are indicated with text. Stimuli are indicated in the upper left corner.

Sorrells et al. Figure 1

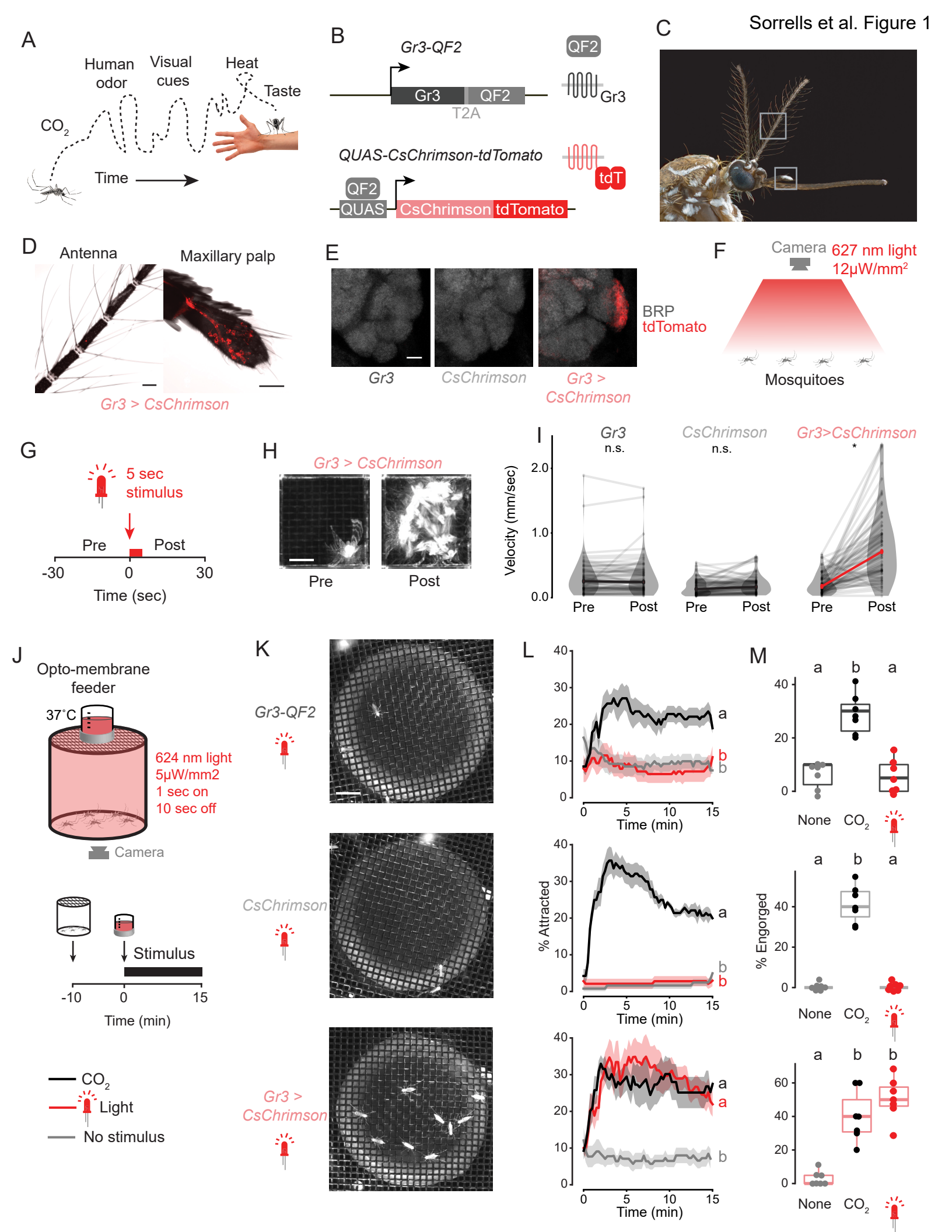

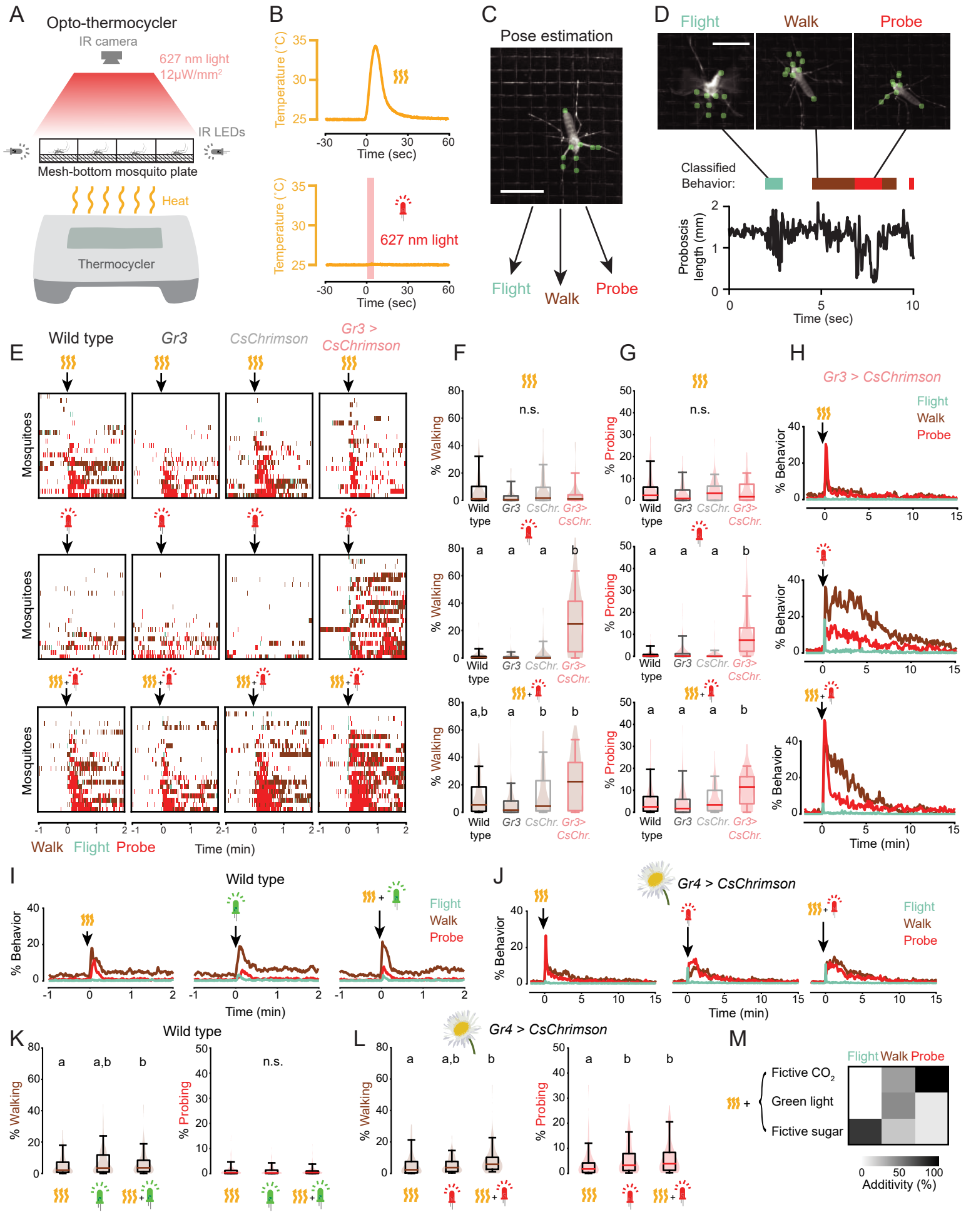
A
Opto-thermocycler
IR camera
627 nm light
12μW/mm²
IR LEDs
Mesh-bottom mosquito plate
Heat
Thermocycler
B
Temperature (°C)
Time (sec)
627 nm light
C
Pose estimation
Flight
Walk
Probe
D
Flight
Walk
Probe
Classified Behavior:
Proboscis length (mm)
Time (sec)
E
Wild type
Gr3
CsChrimson
Gr3 > CsChrimson
Mosquitoes
Walk
Flight
Probe
Time (min)
F
% Walking
n.s.
Wild type
Gr3
CsChr.
Gr3> CsChr.
G
% Probing
H
Gr3 > CsChrimson
% Behavior
I
Wild type
J
Gr4 > CsChrimson
K
Wild type
L
Gr4 > CsChrimson
M
Fictive CO2
Green light
Fictive sugar
Additivity (%)

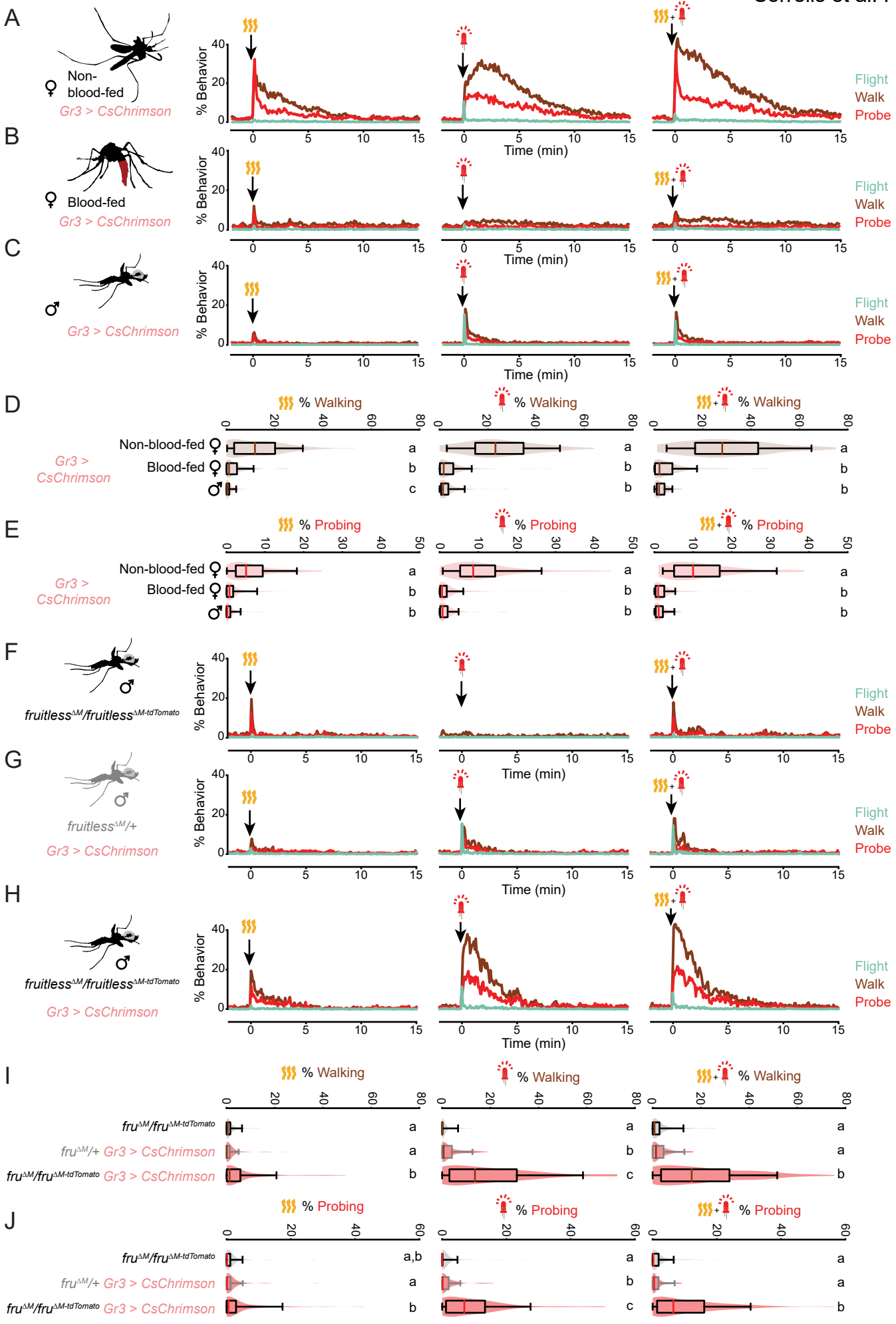
A
Non-blood-fed
Gr3 > CsChrimson
B
Blood-fed
Gr3 > CsChrimson
C
Gr3 > CsChrimson
% Behavior
Time (min)
Flight
Walk
Probe
D
% Walking
Non-blood-fed
Blood-fed
Gr3 > CsChrimson
E
% Probing
F
fruitless^ΔM/fruitless^ΔM-tdTomato
G
fruitless^ΔM/+
Gr3 > CsChrimson
H
fruitless^ΔM/fruitless^ΔM-tdTomato
Gr3 > CsChrimson
I
% Walking
fru^ΔM/fru^ΔM-tdTomato
fru^ΔM/+ Gr3 > CsChrimson
fru^ΔM/fru^ΔM-tdTomato Gr3 > CsChrimson
J
% Probing

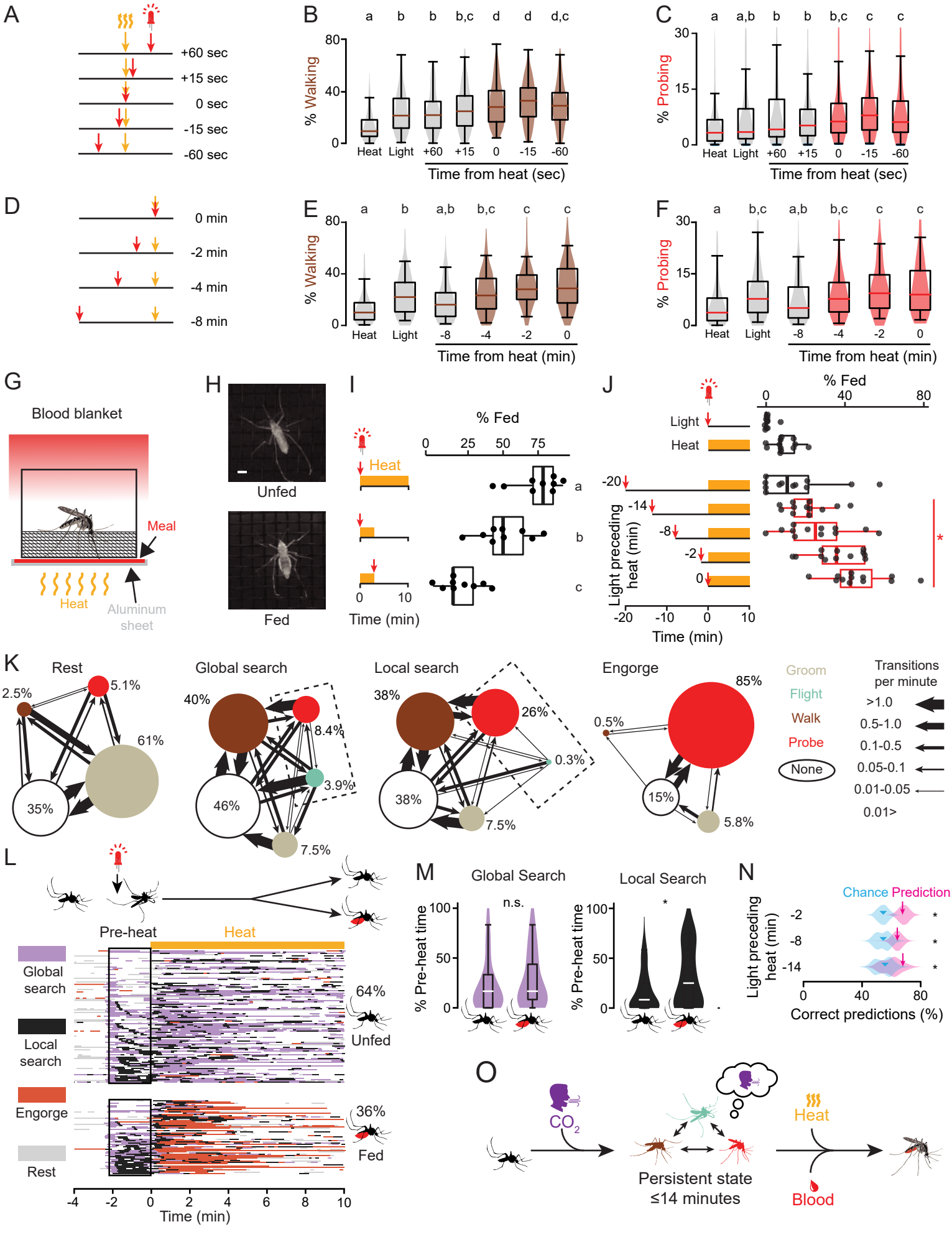
A
+60 sec
+15 sec
0 sec
-15 sec
-60 sec
B
a b b b,c d d d,c
% Walking
Heat Light +60 +15 0 -15 -60
Time from heat (sec)
C
a a,b b b b,c c c
% Probing
Heat Light +60 +15 0 -15 -60
Time from heat (sec)
D
0 min
-2 min
-4 min
-8 min
E
a b a,b b,c c c
% Walking
Heat Light -8 -4 -2 0
Time from heat (min)
F
a b,c a,b b,c c c
% Probing
Heat Light -8 -4 -2 0
Time from heat (min)
G
Blood blanket
Meal
Heat
Aluminum sheet
H
Unfed
Fed
I
% Fed
Heat
a
b
c
Time (min)
J
% Fed
Light
Heat
-20
-14
-8
-2
0
Light preceding heat (min)
Time (min)
K
Rest
Global search
Local search
Engorge
Groom
Flight
Walk
Probe
None
Transitions per minute
>1.0
0.5-1.0
0.1-0.5
0.05-0.1
0.01-0.05
0.01>
L
Pre-heat
Heat
Global search
Local search
Engorge
Rest
64%
Unfed
36%
Fed
Time (min)
M
Global Search
Local Search
n.s.
% Pre-heat time
N
Chance Prediction
Light preceding heat (min)
Correct predictions (%)
O
CO2
Persistent state ≤14 minutes
Heat
Blood

A

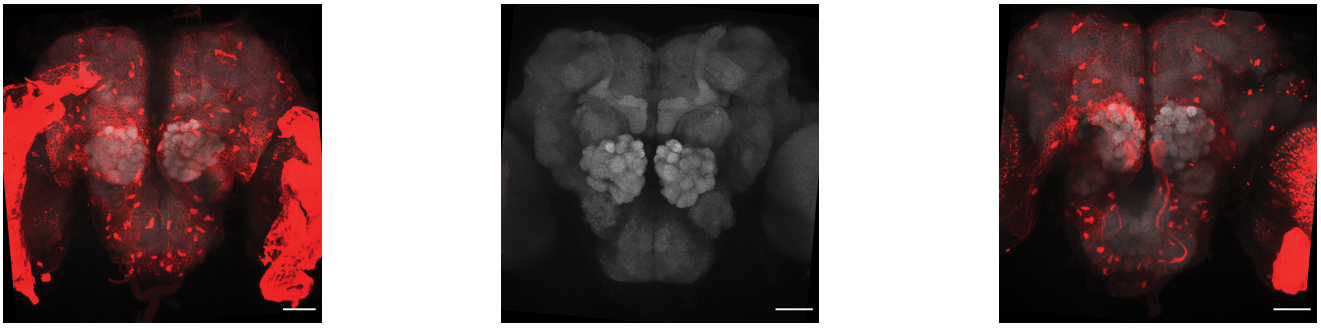

Gr3-QF2
(marker: 3x3P-dsRed)

QUAS-CsChrimson:tdTomato
(marker: 3X3P-ECFP)

Gr3-QF2
(marker: 3XP3-dsRed)
QUAS-CsChrimson:tdTomato
(marker: 3XP3-ECFP)

B

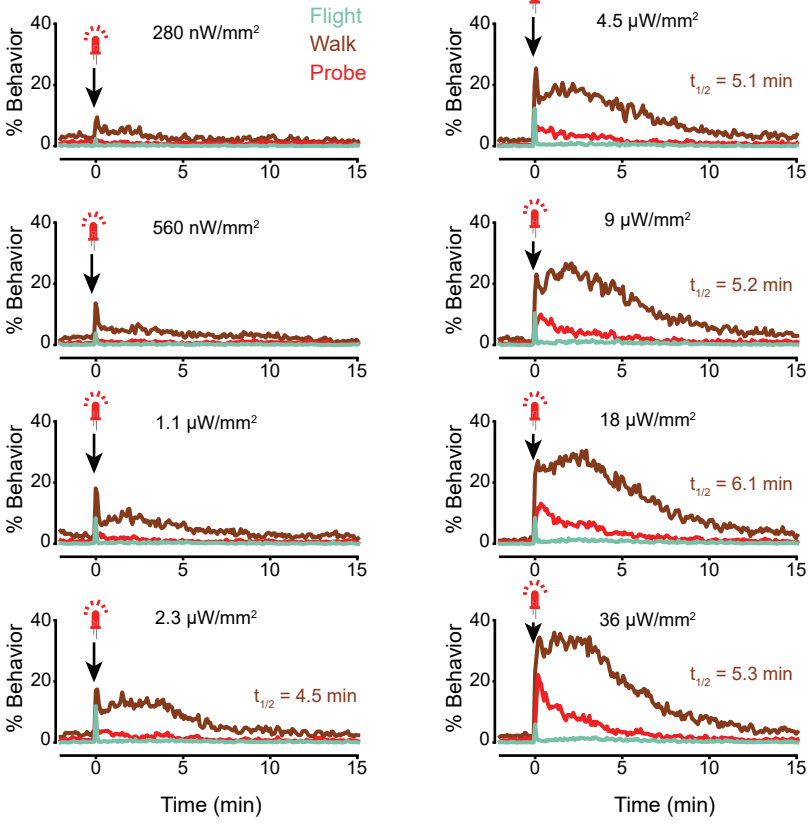

C

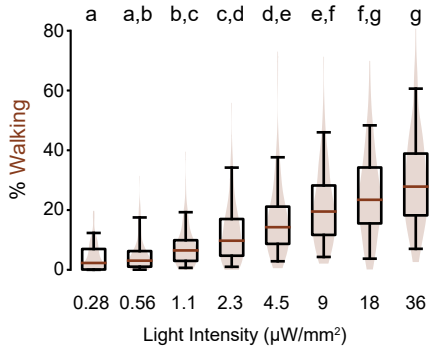

D

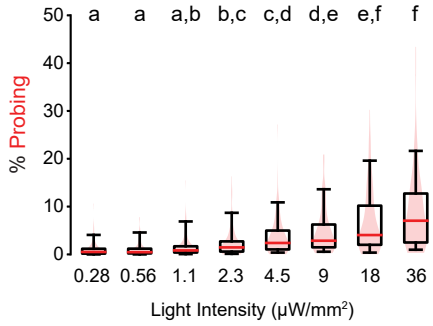

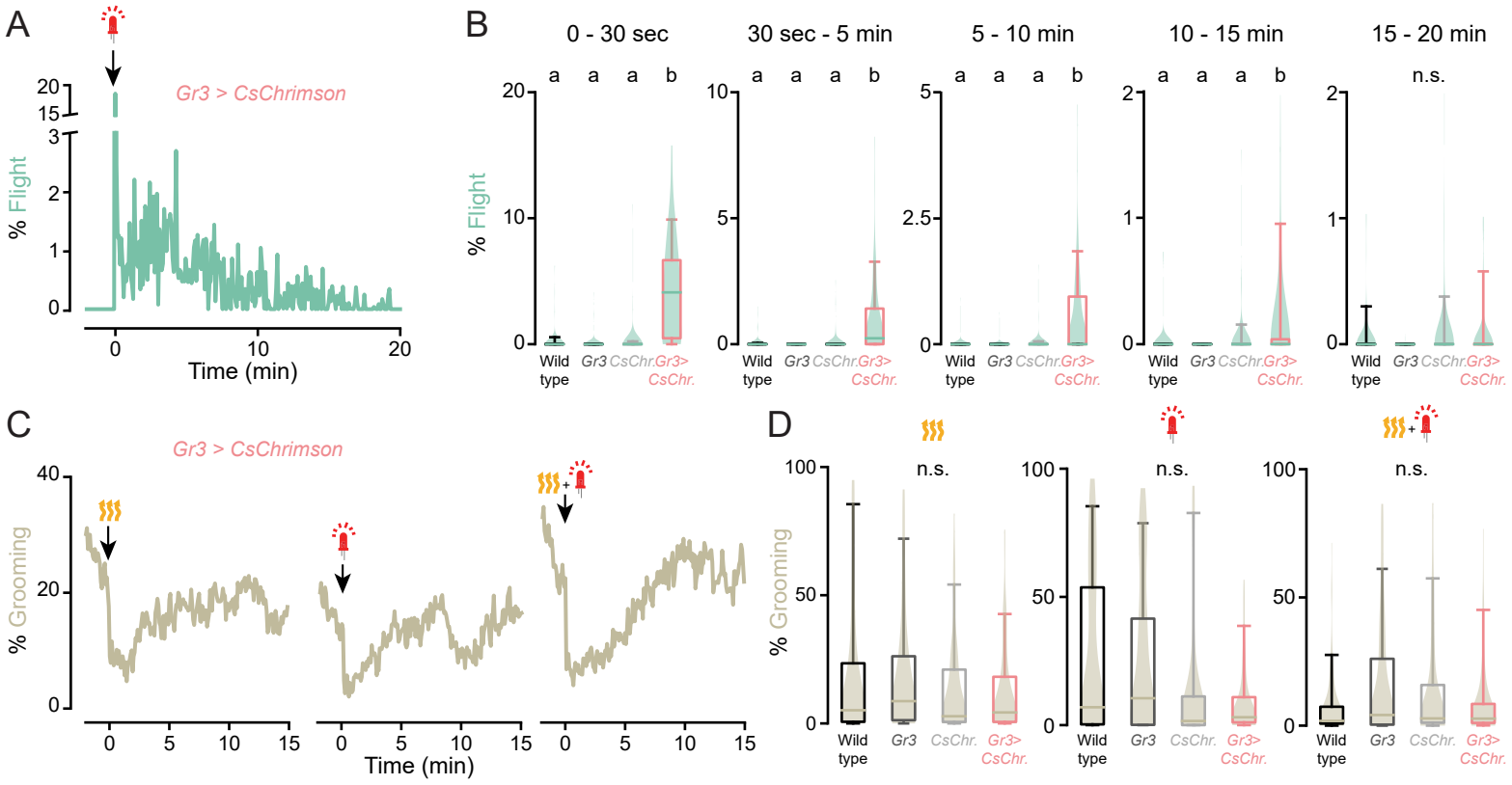
A
Gr3 > CsChrimson
% Flight
Time (min)
B
0 - 30 sec
30 sec - 5 min
5 - 10 min
10 - 15 min
15 - 20 min
a a a b
n.s.
% Flight
Wild type
Gr3
CsChr.
Gr3> CsChr.
C
Gr3 > CsChrimson
% Grooming
Time (min)
D
n.s.
% Grooming
Wild type
Gr3
CsChr.
Gr3> CsChr.

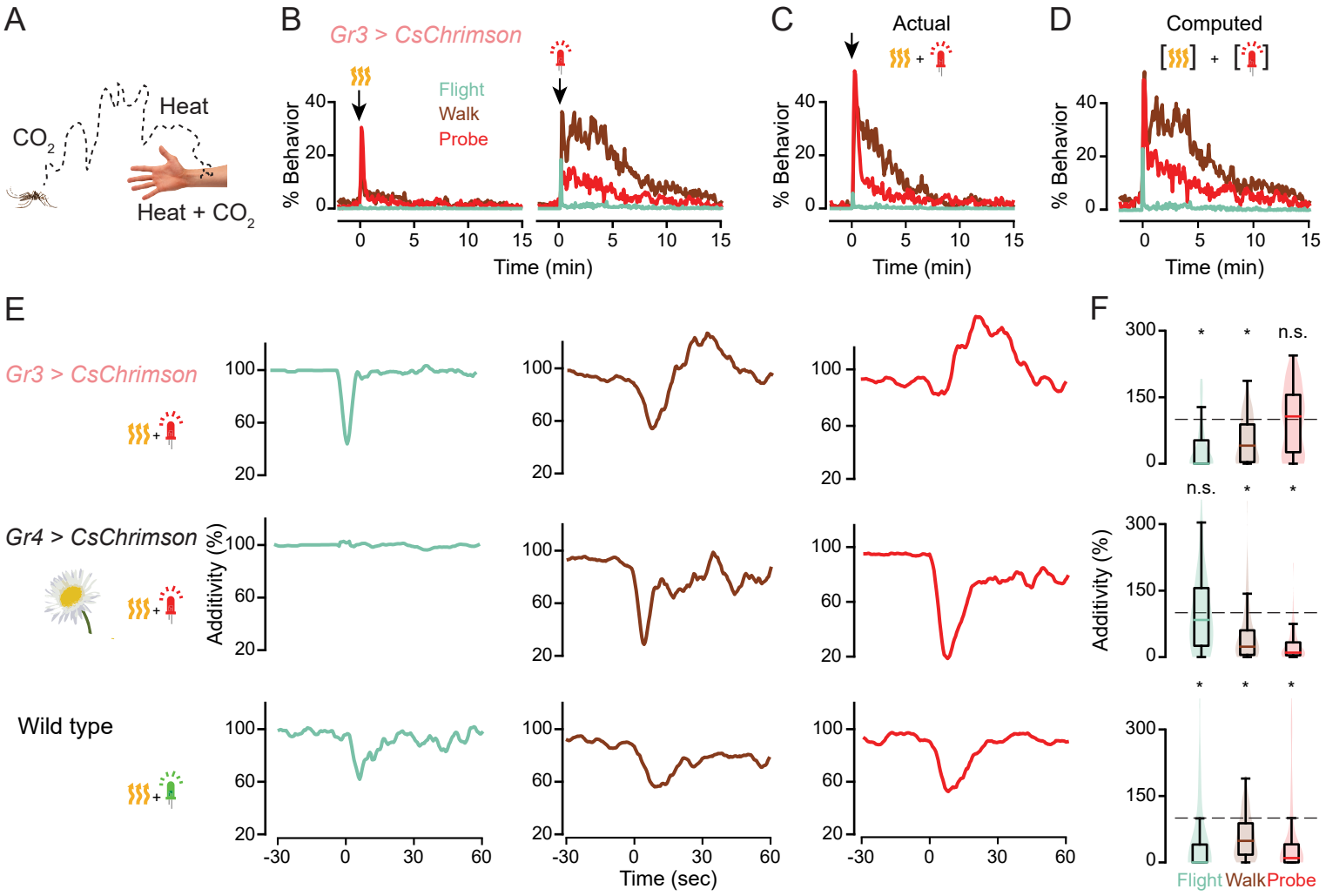
A
CO2
Heat
Heat + CO2
B
Gr3 > CsChrimson
Flight
Walk
Probe
% Behavior
Time (min)
C
Actual
% Behavior
Time (min)
D
Computed
% Behavior
Time (min)
E
Gr3 > CsChrimson
Gr4 > CsChrimson
Wild type
Additivity (%)
Time (sec)
F
Additivity (%)
n.s.
Flight
Walk
Probe

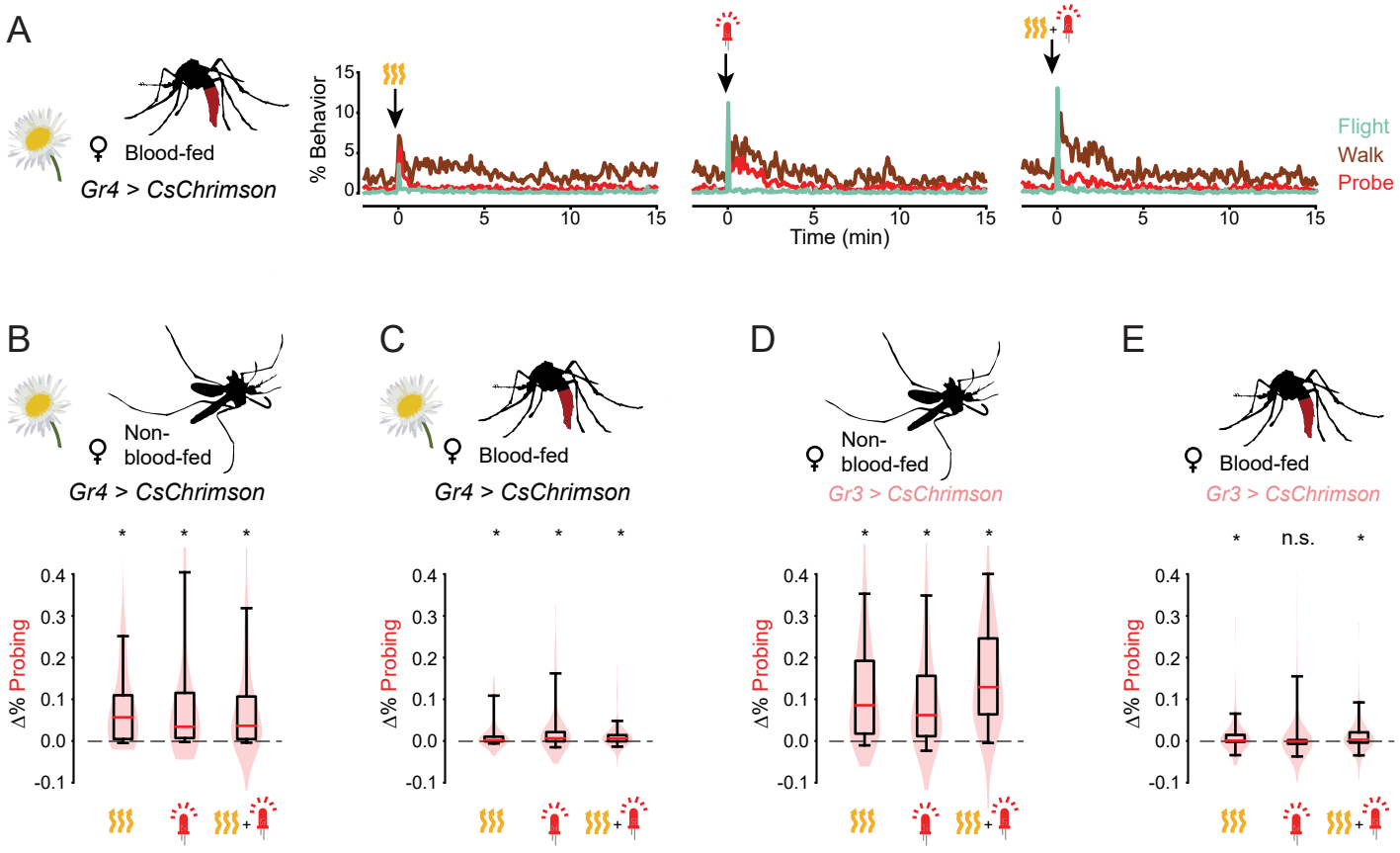
A
Blood-fed
Gr4 > CsChrimson
% Behavior
Time (min)
Flight
Walk
Probe
B
Non-
blood-fed
Gr4 > CsChrimson
C
Blood-fed
Gr4 > CsChrimson
D
Non-
blood-fed
Gr3 > CsChrimson
E
Blood-fed
Gr3 > CsChrimson
Δ% Probing
n.s.

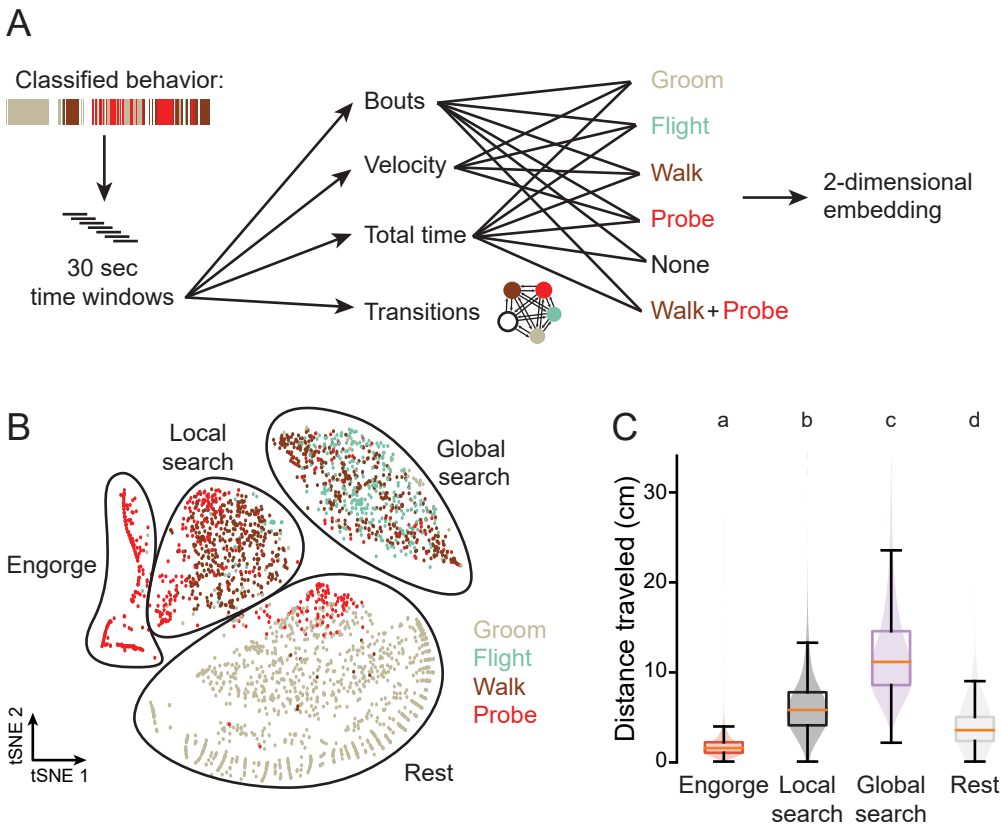
A
Classified behavior:
30 sec
time windows
Bouts
Velocity
Total time
Transitions
Groom
Flight
Walk
Probe
None
Walk + Probe
2-dimensional
embedding
B
Local
search
Global
search
Engorge
Groom
Flight
Walk
Probe
Rest
tSNE 2
tSNE 1
C
a
b
c
d
Distance traveled (cm)
0
10
20
30
Engorge
Local
search
Global
search
Rest

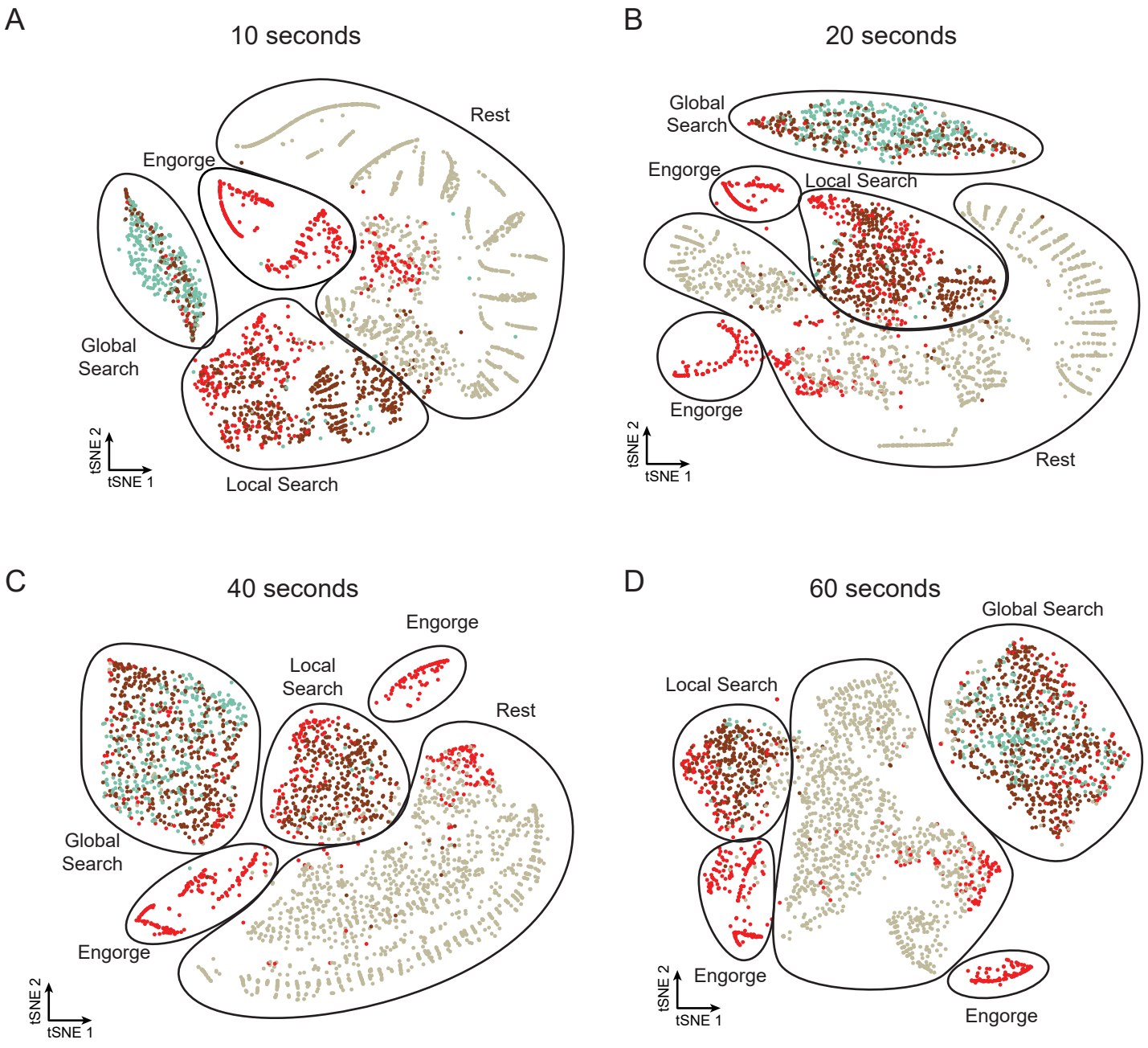
A
10 seconds
Rest
Engorge
Global Search
Local Search
tSNE 2
tSNE 1
B
20 seconds
Global Search
Engorge
Local Search
Engorge
Rest
tSNE 2
tSNE 1
C
40 seconds
Engorge
Local Search
Rest
Global Search
Engorge
tSNE 2
tSNE 1
D
60 seconds
Global Search
Local Search
Engorge
Engorge
tSNE 2
tSNE 1